Received: 14 October 2016 | Revised: 17 January 2017 | Accepted: 18 January 2017

DOI: 10.1002/cne.24177

RESEARCH ARTICLE

WILEY The Journal of Comparative Neurology

Connectivity and ultrastructure of dopaminergic innervation of the inner ear and auditory efferent system of a vocal fish

Jonathan T. Perelmuter[1,4] | Paul M. Forlano[1,2,3,4,5]

[1]Program in Behavioral and Cognitive Neuroscience, The Graduate Center, City University of New York, New York, New York 10016

[2]Program in Ecology, Evolutionary Biology and Behavior, The Graduate Center, City University of New York, New York, New York 10016

[3]Program in Neuroscience, The Graduate Center, City University of New York, New York, New York 10016

[4]Department of Biology, Brooklyn College, City University of New York, Brooklyn, New York 11210

[5]Aquatic Research and Environmental Assessment Center, Brooklyn College, Brooklyn NY, New York 11210

Correspondence
Jonathan T. Perelmuter, Behavioral & Cognitive Neuroscience, Psychology, The Graduate Center, City University of New York, 365 5th Avenue, New York, NY 10016.
Email: jperelmuter@gradcenter.cuny.edu

Funding information
National Institutes of Health, Grant number: SC2DA034996; Professional Staff Congress of the City University of New York, National Science Foundation, Grant number: IOS 1456743 to PMF; Grant numbers: 65650-00 43 and 68877-00 46 to PMF; Doctoral Student Research Grant from the Graduate Center of the City University of New York to JTP; Preliminary data for this project was collected at the Marine Biological Laboratory in Woods Hole, MA as part of a Whitman Center Research Award to PMF.

Abstract

Dopamine (DA) is a conserved modulator of vertebrate neural circuitry, yet our knowledge of its role in peripheral auditory processing is limited to mammals. The present study combines immunohistochemistry, neural tract tracing, and electron microscopy to investigate the origin and synaptic characteristics of DA fibers innervating the inner ear and the hindbrain auditory efferent nucleus in the plainfin midshipman, a vocal fish that relies upon the detection of mate calls for reproductive success. We identify a DA cell group in the diencephalon as a common source for innervation of both the hindbrain auditory efferent nucleus and saccule, the main hearing endorgan of the inner ear. We show that DA terminals in the saccule contain vesicles but transmitter release appears paracrine in nature, due to the apparent lack of synaptic contacts. In contrast, in the hindbrain, DA terminals form traditional synaptic contacts with auditory efferent neuronal cell bodies and dendrites, as well as unlabeled axon terminals, which, in turn, form inhibitory-like synapses on auditory efferent somata. Our results suggest a distinct functional role for brain-derived DA in the direct and indirect modulation of the peripheral auditory system of a vocal nonmammalian vertebrate.

KEYWORDS

auditory efferents, dopamine, electron microscopy, hearing, immunohistochemistry, RRID: AB_90650, RRID: AB_2201528, RRID: 22806, teleost

1 | INTRODUCTION

Efferent control is an important feature of sensory systems but remains less well understood than afferent pathways. Nearly all vertebrates examined to date possess a cholinergic efferent innervation of the inner ear that originates in the hindbrain (Köppl, 2011), with proposed functions that include protection from overstimulation, homeostasis, selective attention, signal detection, and sound source localization (Andéol et al., 2011; Darrow, Maison, & Liberman, 2006; Robertson, 2009; Smith & Keil, 2015; Terreros, Jorratt, Aedo, Elgoyhen, & Delano, 2016; Tomchik & Lu, 2006b). While cholinergic auditory efferents are well studied across vertebrate taxa, comparatively less attention has been given to dopamine (DA) as a modulator of peripheral hearing (Gil-Loyzaga, 1995). DA fibers and receptors have been localized within the rodent cochlea (Darrow, Simons, Dodds, & Liberman, 2006; Maison et al., 2012), but studies examining DA innervation of auditory endorgans of anamniotes are limited to a single species of teleost fish (Forlano, Kim, Krzyminska, & Sisneros, 2014; Forlano, Ghahramani

et al., 2015) and investigations of the ultrastructure of DA terminals are limited to guinea pig (d'Aldin et al., 1995; Eybalin, Charachon, & Renard, 1993). The function of DA in the cochlea, as suggested by studies in rodents, is to protect against acoustic trauma (Lendvai et al., 2011; Maison et al., 2012; Ruel et al., 2001), but other hypotheses, such as signal detection and sound source localization, have not been tested. The potential modulatory role of DA in the auditory periphery in the context of natural behaviors remains unexplored.

The plainfin midshipman fish, *Porichthys notatus*, is an excellent model organism for investigating neural mechanisms of vocal-acoustic behavior, with well-characterized ascending and descending auditory pathways (Bass, Bodnar, & Marchaterre, 2000; Bass, Marchaterre, & Baker, 1994; Goodson & Bass, 2002). During the summer breeding season, type I males migrate from the benthic zone to intertidal nesting sites along the northwestern coast of North America where they produce nocturnal hum-like vocalizations that attract females for mating opportunities. Type II males do not build nests or court females but rather sneak fertilization opportunities (Bass, 1996; Brantley & Bass, 1994). All adult morphs (type Is, females and type II males) undergo seasonal and steroid dependent changes in the auditory periphery, resulting in lower hearing thresholds and improved encoding of social signals in the summer, specifically within the range of the upper harmonics of the male vocalization (Bhandiwad, Whitchurch, Colleye, Zeddies, & Sisneros, 2017; Forlano, Maruska, Sisneros, & Bass, 2016; Rohmann & Bass, 2011; Sisneros & Bass, 2003; Sisneros, Forlano, Deitcher, & Bass, 2004). This likely improves detection of the courtship call, as the upper harmonics propagate farther in the shallow water of the intertidal zone (Bass & Clark, 2003; Fine & Lenhardt, 1983). Mechanisms for this plasticity include an increase in the number of sensory receptors, that is, hair cells, in the inner ear (Coffin, Mohr, & Sisneros, 2012), as well an upregulation in the number of calcium-activated potassium (BK) channels in hair cells (Rohmann, Fergus, & Bass, 2013). It has also been suggested that centrifugal modulation could mediate plasticity (Forlano, Sisneros, Rohmann, & Bass, 2015; Sisneros & Bass, 2003). The saccule, the main endorgan of hearing in midshipman (Cohen & Winn, 1967) and most teleosts (Popper & Fay, 1999), receives tyrosine hydroxylase (TH, enzyme for catecholaminergic synthesis) innervation from the periventricular posterior tuberculum (TPp) in the diencephalon (Forlano et al., 2014, Figure 1a, b), a proposed homolog of the mammalian A11 DA cell group (Schweitzer, Lohr, Filippi, & Driever, 2012; Yamamoto & Vernier, 2011). The saccule also receives cholinergic efferent innervation from the octavolateralis efferent nucleus (OE) in the hindbrain (Bass et al., 1994, 2000; Brantley & Bass, 1988; Forlano et al., 2014, Forlano, Ghahramani et al., 2015; Weeg, Land, & Bass, 2005). While the OE projects to all inner ear endorgans and the lateral line in teleosts (Köppl, 2011; Roberts & Meredith, 1992; Tomchik & Lu, 2006a), we here refer to it interchangeably as the auditory efferent system (after Chagnaud & Bass, 2013) as backfills from the saccule fill a majority of OE neurons in midshipman (Bass et al., 1994, 2000; Forlano et al., 2014). Importantly, the OE receives prominent TH fibers and puncta that appear to also originate from the TPp (Forlano et al., 2014, Figure 1a, c). We have recently demonstrated that the putatively dopaminergic innervation of the midshipman saccule changes seasonally, as does the putatively dopaminergic input to the OE (Forlano, Ghahramani et al., 2015). Furthermore, playbacks of courtship calls to type I males activate catecholaminergic neurons in the TPp (Petersen et al., 2013), suggesting that socially salient acoustic stimuli elicit DA release in both the saccule and OE.

The goal of the present study was to use neuroanatomical tract tracing, immunohistochemistry and electron microscopy to investigate the fine structure of DA innervation of the saccule and the OE. We tested the following hypotheses: (a) the OE receives DA input from the TPp, the same source as the saccule; (b) DA innervation of the saccule is regionally homogenous; and (c) DA terminals will be found in proximity to, or making synaptic contact with hair cells and neuronal processes in the saccule and the neurons in the OE. Our results show that a single dopaminergic cell group in the midshipman diencephalon is extensively connected to the peripheral and hindbrain efferent auditory system and therefore capable of coordinated modulation of hearing during natural behaviors.

2 | MATERIALS AND METHODS

2.1 | Animals

Animals ($n = 32$) were collected during the summer from intertidal breeding sites in Tomales Bay, CA and near Brinnon, WA or during the winter, by otter trawl, in Puget Sound, WA. Quantitative sex or seasonal differences in catecholamine-specific connectivity or ultrastructure were not measured in the present study. Animal acquisition and experimental procedures were approved by the Institutional Animal Care and Use Committee of Brooklyn College, Brooklyn, NY.

2.2 | Tissue preparation

Fish were anesthetized in 0.025% benzocaine (Sigma Chemicals, St Louis, MO), transcardially perfused with teleost's ringers, followed by 4% paraformaldehyde, or 1.5–2.5% paraformaldehyde, and 0.5–2.5% glutaraldehyde (for electron microscopy, EM), in 0.1 M phosphate buffer (PB, pH 7.2). Variations in the amount of glutaraldehyde in the perfusion fixative did not have any effect on the antigenicity of the TH antibody. Brains and saccules were dissected out and post-fixed for 1 hr and stored in 0.1 M PB with 0.3% sodium azide at 4 °C. Prior to storage, saccular epithelia (SE) were dissected off the otolith and most of the extra-epithelial membrane was trimmed away. Brains and a subset of SEs were incubated in 30% sucrose in PB for 24 to 48 hr, then sectioned in the transverse (brains) or sagittal (SEs) plane on a Leica CM1850 cryostat (Nussloch, Germany) at 25 μm (brains) or 20 μm (SEs) and collected onto Superfrost plus (VWR, Radnor, PA) slides (for fluorescent immunohistochemistry) or 60 μm and collected in well-plates containing 0.1 M PB (for immuno-EM).

2.3 | Neuroanatomical tract tracing

Brains were embedded in 3% agarose, mounted in a Lancer 1000 vibratome (Vibratome Company, St. Louis, MO) and sectioned rostrally from the caudal hindbrain to the level of the OE in the medulla ($n = 6$).

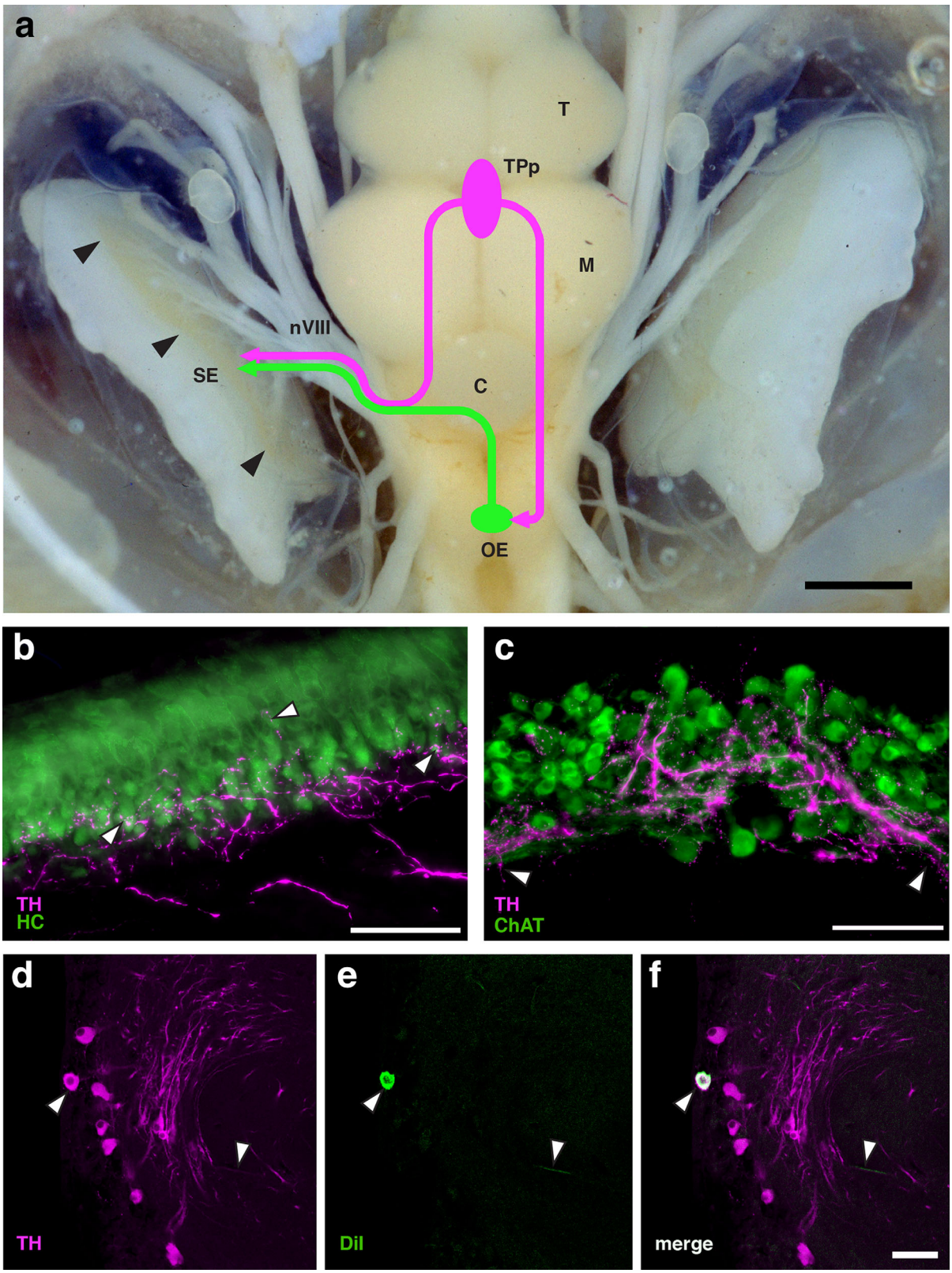

FIGURE 1 (a) Dorsal view of midshipman brain and inner ear depicting the two efferent nuclei, the dopaminergic periventricular posterior tuberculum (TPp, purple) and the cholinergic octavolateralis efferent nucleus (OE, green), which project to the saccular epithelium (SE, black arrowheads, the main hearing endorgan) via the eighth nerve (nVIII). Fluorescent micrographs depict tyrosine hydroxylase immunoreactive (TH-ir) innervation of midshipman saccule and OE (b, c). (b) TH-ir fibers (purple) enter the base of the SE and form punctate swellings (white arrowheads) around the base of hair cells (HC, green). (c) Punctate TH-ir fibers extensively wrap around OE neurons (identified with antibody for choline-acetyltransferase, ChAT, green) and bundles of laterally projecting dendrites (white arrowheads). (d–f) DiI implants into OE result in filled cells and fibers (green, white arrowheads) in the TPp. DiI-filled cells in TPp are also TH-ir (f), confirming a dopaminergic projection to the OE (a). Additional abbreviations in (a): *C* cerebellum, *M* midbrain, *T* telencephalon. (a, b), modified from Forlano and Sisneros (2016). Scale bar = 1.5 mm in (a) 50 μm in (b–f)

TABLE 1 Primary antibodies used

Name	Immunogen	Manufacturer	RRID	Type	Species	Dilution
Anti-ChAT	Choline acetyltransferase purified from human placenta	Millipore, #AB144	AB_90650	polyclonal	goat	1:200
Anti-DBH	Dopamine-beta-hydroxylase purified from bovine adrenal medulla	ImmunoStar, #22806	22806	polyclonal	rabbit	1:2,000
Anti-TH	Tyrosine hydroxylase purified from PC12 cells	Millipore, #MAB318	AB_2201528	monoclonal	mouse	1:1,000

Under a dissecting microscope, crystals of 1,1-dioctadecyl-3,3,3,3-tetramethyl-indocarbocyanine perchlorate (DiI; Thermo Fisher Scientific, Waltham, MA) were applied via minutien pin to OE somata, visualized with methylene blue. Crystal size was selected to contact a majority of the exposed bilateral extent of the nucleus. The applied crystals were sealed with 3% agarose and brains were incubated in 4% paraformaldehyde for 21–24 days in the dark at 37 °C. Brains were then sectioned in the transverse plane at 50–100 μm on the vibratome, mounted on glass slides in 0.1 M PB, cover slipped with ProLong Gold (Thermo Fisher Scientific) and immediately imaged. In a subset of animals ($n = 2$), sections containing DiI backfilled cells were processed for TH immunohistochemistry (see below).

2.4 | Fluorescent immunohistochemistry

Brain sections on slides or free floating as well as whole SEs were processed as follows: 2 × 10 min in 0.1 M phosphate-buffered saline (PBS, pH 7.2), 1 hr in blocking solution [(10% normal donkey serum (Jackson ImmunoResearch, West Grove, PA) + 0.3% Triton X-100 in PBS)], 18 hr in the following primary antibodies diluted in blocking solution: monoclonal mouse anti-TH (Millipore, Billerica, MA, #MAB318, RRID: AB_2201528) diluted 1:1,000; polyclonal rabbit anti-dopamine beta hydroxylase (DBH, Immunostar, Hudson, WI, USA, #22806, RRID: 22806) diluted 1:2,000, and polyclonal goat anti-choline acetyltransferase (ChAT, Millipore, #AB144, RRID: AB_90650) diluted 1:200. Tissue was washed 6 × 10 min in PBS + 0.5% donkey serum and incubated for 2 hr in the following secondary antibodies (Thermo Fisher Scientific) diluted 1:200 in blocking solution: anti-mouse Alexa Flour 488, anti-rabbit or anti-goat 568, and anti-goat 680. Tissue was then washed 3 × 10 min in PBS. Whole mount saccules were mounted onto slides. All slides were cover slipped with ProLong Gold containing 4,6-diamidino-2-phenylindole nuclear stain (DAPI; Thermo Fisher Scientific). For free floating sections containing DiI filled cells, Triton X-100 in the blocking solution was replaced with 0.1% digitonin. All incubations and washes were carried out at room temperature.

2.5 | Antibody characterization

Table 1 lists the immunogen, manufacturer, RRID number, species and dilution for all primary antibodies utilized in this study. The goat polyclonal anti-ChAT antibody was produced against whole choline acetyltransferase purified from human placental lysate and western blot analysis shows bands of 68–70 kDa in mouse brain extract (manufacturer's information). Comparative western blot analysis shows similar bands of 68–72 kDa in the African clawed frog (López, Perlado, Morona, Northcutt, & González, 2013) and a diverse group of fishes, including lesser spotted dogfish, sturgeon, trout (Anadón et al., 2000), and Senegal bichir (López et al., 2013). The pattern of labeling in the midshipman fish is comparable to that reported in a broad range of nonmammalian vertebrates where the antibody has been well characterized and used to describe cholinergic neurons and fibers that are generally conserved across vertebrates (Rodríguez-Moldes et al., 2002). It labels cholinergic cranial nerve motor neurons, auditory efferent neurons and fibers in amphibians (Marín, Smeets, & González, 1997), bichir (López et al., 2013), dogfish (Anadón et al., 2000), lamprey (Pombal, Marín, & González, 2001), lizard (Wibowo, Brockhausen, & Köppl, 2009), pigeon (Medina & Reiner, 1994), rainbow trout (Pérez et al., 2000), red-eared turtle (Jordan, Fettis, & Holt, 2015), sturgeon (Adrio, Anadón, & Rodríguez-Moldes, 2000), and zebrafish (Mueller, Vernier, & Wullimann, 2004). A previous study in midshipman using a different monoclonal anti-ChAT antibody (Brantley & Bass, 1988) reported identical labeling in hindbrain neurons and fibers. Omission of primary or secondary antibodies resulted in absence of labeling.

The immunogen for the rabbit polyclonal anti-DBH antibody was purified DBH from bovine adrenal medulla and recognizes a triplet of 72–74 kDa in rat brain extract on western blot (manufacturer's information). This antibody has been previously used to identify noradrenergic neurons and fibers in the brains of rodents (Bullman, Hartig, Holzer, & Arendt, 2010; Tsuneoka et al. 2013), birds (Castelino & Ball, 2005; Pawlisch, Kelm-Nelson, Stevenson, & Riters, 2012), and in the peripheral nervous system of turtle (Belfry & Cowan, 1995) and hachetfish (Zaccone et al., 2011). In the present study, in midshipman, this DBH antibody labels neurons with a position and morphology in the locus coeruleus (LC) that is consistent with LC noradrenergic (NA) neurons found in all vertebrates examined to date (Smeets & González, 2000). These highly conserved LC NA neurons have been identified via a combination of different TH and DBH antibodies in brown ghost knifefish (Sas, Maler, & Tinner, 1990), filefish (Funakoshi et al., 2002), goldfish (Hornby & Piekut, 1990), lamprey (Pierre, Mahouche, Suderevskaya, Repérant, & Ward, 1997), sturgeon (Adrio, Anadón, & Rodríguez-Moldes, 2002), three-spined stickleback (Ekström, Honkanen, & Borg, 1992), and zebrafish (Kaslin & Panula, 2001; Ma, 1994, 1997; McLean & Fetcho, 2004). Importantly, in both the aforementioned citations and in our study, DBH does not label TH-ir neurons in the diencephalon, which are considered to be dopaminergic (Yamamoto & Vernier, 2011). Furthermore, LC neurons, but not diencephalic TH-ir neurons, express DBH mRNA in zebrafish (Guo et al., 1999) and NA transporter mRNA

in medaka (Roubert et al., 2001). Conversely, diencephalic TH-ir neurons, but not LC neurons, express DA transporter mRNA in zebrafish (Holzschuh, Ryu, Aberger, & Driever, 2001). For comparison, we tested the DBH antibody used in the present study in cryosections of larval zebrafish and found an identical pattern of TH-ir/DBH-ir neurons in the LC, but only TH-ir neurons in the diencephalon. Omission of primary or secondary antibodies resulted in absence of labeling.

The immunogen for the mouse monoclonal anti-TH antibody was purified from PC12 cells and western blot analysis of both rat and fish brain lysate show comparable expected bands of ~59–63 kDa and no cross-reactivity with other structurally similar enzymes (Adrio et al., 2002; Goebrecht, Kowtoniuk, Kelly, & Kittelberger, 2014; manufacturer's information). The antibody labels an expected pattern consistent with known catecholaminergic neurons and fibers in plainfin midshipman (Forlano et al., 2014; Goebrecht et al., 2014), other teleosts (McLean & Fetcho, 2004; Tay, Ronneberger, Ryu, Nitschke, & Driever, 2011) and across vertebrates (Smeets & González, 2000).

2.6 | Fluorescent image acquisition and analysis

Sectioned brain tissue ($n = 6$) was imaged on an Olympus BX61 epifluorescence compound microscope (Tokyo, Japan) with a 20× objective, DAPI, GFP, Texas Red, and Ultra Far Red filters (Chroma, Bellow Falls, VT), and acquired with Metamorph imaging software (Molecular Devices, Sunnyvale, CA). Photomicrographs were projections compiled from 5 to 10 μm z-stacks. All SE images were acquired on a Nikon D-Eclipse C1 confocal microscope and EZ-C1 software (Tokyo, Japan). Whole mounts ($n = 4$) were imaged at 10× with a resolution of 1024 × 1024 pixels using a 40 μm z-stack and 1 μm step size. Composite images of whole mounts were created with Photoshop CS 6 (Adobe, San Jose, CA). For quantitative analysis of efferent innervation of the saccule, images from sagittal sections through SE were acquired with a 60x oil-immersion objective, 2× digital zoom, 1024 × 1024 pixel resolution and 60 μm z-stacks with a 0.25 μm step size. 20 images equally distributed across the rostro-caudal and dorso-ventral extent of the SE were acquired from each animal (females in summer reproductive condition, $n = 4$). Each image was categorized as being in the rostral, medial or caudal division of the SE. Putative TH-immunoreactive (-ir) and ChAT-ir puncta were measured and analyzed as described previously (Forlano, Ghahramani et al., 2015). Statistical analysis and graphs were produced using GraphPad Prism 6 (La Jolla, CA). All multi-labeled fluorescent images were acquired sequentially.

2.7 | Immunohistochemistry and imaging for EM

Free floating whole SE and 60 μm sections from the brain containing the OE ($n = 13$) were washed 2 × 10 min in 0.1 M PBS and then blocked in 0.1 M PBS + 5% normal donkey serum + 0.3% dimethyl sulfoxide (Sigma Chemicals) for 1 hr. All incubations and washes were carried out at room temperature on a rotator. Mouse anti-TH (Millipore, #MAB318, RRID: AB_2201528) was diluted in blocking solution (1:1,000) and all tissue was incubated in sealed glass vials for 16 hr. After primary incubation, the tissue was washed 6 × 10 min in PBS + 0.5% donkey serum (PBS-DS).

Secondary biotinylated anti-mouse antibody (Vector Labs, Burlingame, CA) was diluted (1:200) in blocking solution and tissue was incubated for 2 hr. Tissue was washed 6 × 10 min in PBS + 0.5% donkey serum (PBS-DS) and incubated for 1 hr in Vectastain ABC solution (Vector Labs) diluted (1:200) in PBS-DS. Tissue was washed 6 × 10 min in 0.1 M PB and then processed with a 3-3′-diaminobenzidine (DAB) peroxidase kit (Vector Labs) for 2–6 min to visualize labeling and provide a substrate for osmification. Tissue was washed 4 × 10 min in 0.1 M PB. SE and OE sections containing visible DAB reaction product were then selected for further processing for EM.

Tissue was rinsed 3 × 5 min in 0.1 M PB, followed by 3 × 5 min in 0.2 M PB, then stained with 1% osmium tetroxide in 0.2 M PB for 45 min. Following washes of 3 × 10 min each in 0.2 M PB, 0.1 M PB and double-distilled water (ddH_2O), tissue was then dehydrated in a graded series of ethanols, infiltrated, and flat-embedded in Eponate resin (Ted Pella, Redding, CA). Embedded SEs were cut into rostral, medial, and caudal regions and re-embedded in coffin molds with the rostro-caudal axis either perpendicular or parallel to the block face. OE sections were mounted on top of coffin molds with the dorso-ventral axis parallel to the block surface.

Semithin sections (500 nm) from resin blocks were taken on a Leica EM UC6 ultramicrotome, visualized with methylene blue and examined under a light microscope. These reference sections were used as guides to trim blocks down to regions of interest. A few additional semithin sections (200 nm) were taken after trimming to confirm isolation of region of interest and to serve as reference sections to EM images. Ultrathin serial sections (60–70 nm, 5–20) were collected onto formvar or pioloform coated copper slot grids and counterstained with 3% uranyl acetate (8 min) and Reynold's lead citrate (5 min).

Grids were imaged at 80 kV with a FEI Morgagni 268 transmission electron microscope (Hillsboro, OR) equipped with a CCD camera and micrographs were acquired using AMT image capture software (Advanced Microscopy Techniques, Woburn, MA). TH-ir profiles were identified by an electron dense, membrane-bounded DAB-osmium-reaction product, which could be observed in at least 2 or more serial sections. Omission of primary antibodies resulted in an absence of labeling. Regions containing TH-ir profiles within the OE and saccule were selected from low magnification images (1,400×) by random systematic sampling for subsequent examination at higher magnifications of up to 89,000×. To evaluate presence of synaptic specializations in the saccule, five TH-ir profiles from each region of SE (rostral, medial & caudal) from three animals were randomly selected, for a total of 45 profiles, and followed through 9–20 serial sections. Images of profiles were acquired at 5,600×–7,100 × and 28,000×–36,000×. Measurements of distance between membranes, profile diameter and synaptic vesicle diameter were made with ImageJ 1.47v (National Institutes of Health, Bethesda, MD) and are presented as ranges. Synapses were defined according to Peters, Palay, and Webster (1991) as close apposition of two membranes with both synaptic vesicles on one side and an even thickening of the two membranes (symmetric) or an uneven thickening on the side without vesicles (asymmetric). EM micrograph contrast adjustment and pseudocoloration was completed with Photoshop CS6 (Adobe).

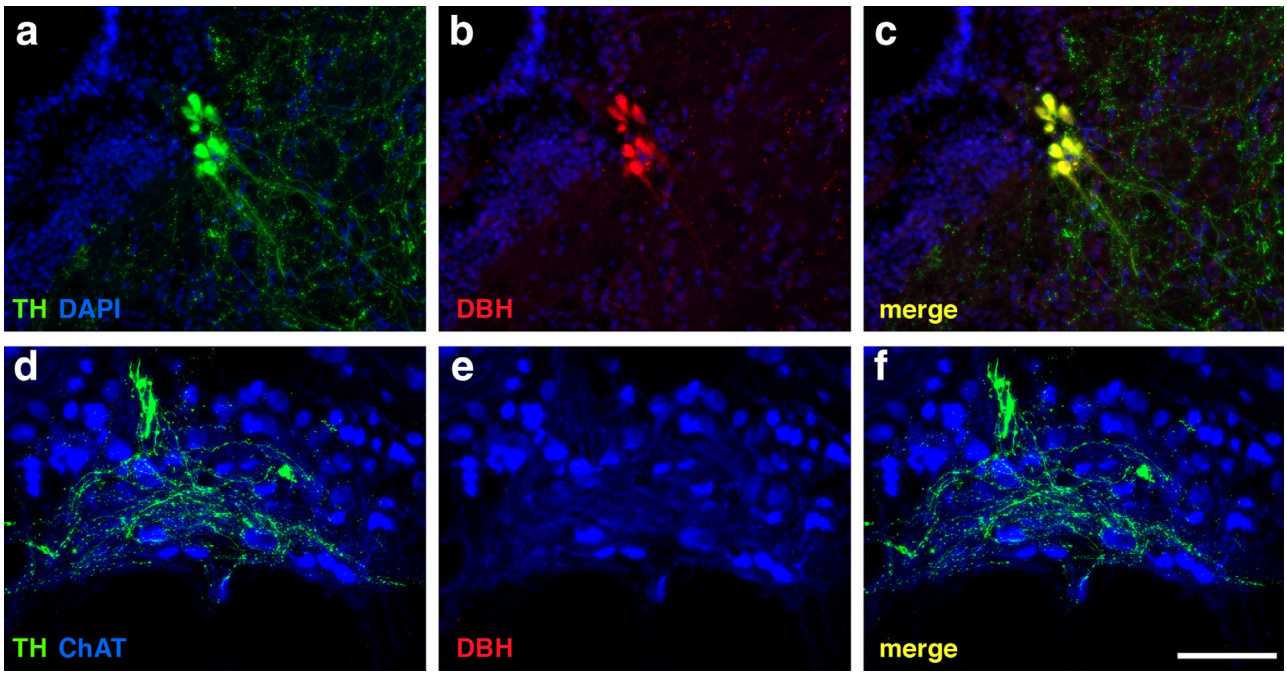

FIGURE 2 Fluorescent micrographs showing combined tyrosine hydroxylase (TH-ir) and dopamine beta hydroxylase (DBH-ir) immunoreactive labeling in the locus coeruleus (LC, a–c) and octavolateralis efferent nucleus (OE, d–f). LC neurons and dendrites are both TH-ir (a, c) and DBH-ir (b, c), indicating the synthesis of noradrenaline. The dense TH-ir fibers in OE (d, f) contain no DBH-ir signal (e, f). Scale bar = 100 μm in (a–f)

3 | RESULTS

3.1 | DiI tract tracing

DiI implants into the OE resulted in filled cells in the region of the TPp (2–8 per animal, mean = 4, $n = 6$). Filled TPp cells are large and pear-shaped, resembling the dopaminergic cell population in this region (Forlano et al., 2014). To confirm the neurochemical identity of filled cells, we used immunohistochemistry for TH in a subset of animals ($n = 2$) and found that all filled TPp cells were TH-ir (2–3 cells per animal, Figure 1d–f). No other filled cells were observed in other catecholaminergic cell groups rostral to the OE.

3.2 | DBH-TH double labeling

The DBH antibody labeled cell groups in the hindbrain in a pattern consistent with previous reports from other vertebrates including teleost fishes (Kaslin & Panula, 2001; Ma, 1997; Smeets & González, 2000). As expected, the LC contains cells and fibers that are both TH-ir and DBH-ir (Figure 2a–c), indicative of noradrenergic-producing neurons. In contrast, TH-ir neurons in TPp are DBH-ir negative (also see Kaslin & Panula, 2001). The OE contains dense TH-ir fibers but is devoid of DBH-ir signal (Figure 2d–f). Likewise, the saccule has robust TH-ir fibers but no DBH-ir signal (not shown).

3.3 | Distribution of efferent innervation in the saccule

Inspection of whole mounts did not reveal any obvious regional differences in dopaminergic or cholinergic innervation patterns (Figure 3a). Analysis of sagittal sections (Figure 3b) revealed no differences between rostral, medial, and caudal regions for TH-ir puncta per section ($F(2,6) = 0.91$, $p = .45$), average TH-ir punctum area ($F(2,6) = 0.29$, $p = .76$), ChAT-ir puncta per section ($F(2,6) = 0.91$, $p = .45$) or average ChAT-ir punctum area ($F(2,6) = 3.98$, $p = .08$) (Figure 3c,d).

3.4 | Synaptology of the saccule

All synaptic contacts with hair cells occur below their nucleus within the basal third of the epithelium, concentrated around the base, and show general features conserved across vertebrate hair cells. Afferent synapses are characterized by a presynaptic ribbon (an electron dense spherical or ovoid structure), numerous presynaptic vesicles surrounding the ribbon and a postsynaptic density (Figure 4a). Efferent synapses, presumably cholinergic and originating from the OE, are characterized by numerous synaptic vesicles in the efferent terminal, and a darkening of the postsynaptic membrane overlying an intracellular envelope known as the subsynaptic cistern (Figure 4b). Less common, but across all subjects, efferent terminals are found making synapses directly on afferent processes. The efferent terminal contains numerous vesicles, but unlike efferent-hair cell synapses, there is no postsynaptic cistern. Instead, the presynaptic efferent terminal shows a membrane density (Figure 4c). Afferent processes are also observed to form close and electron dense membrane oppositions with other afferents. These membrane associations contain no synaptic vesicles and the distance between membranes is 8–12 nm. These junctions are found both between afferent processes below hair cells as well as between postsynaptic afferent profiles (Figure 4d). Gap junctions, with

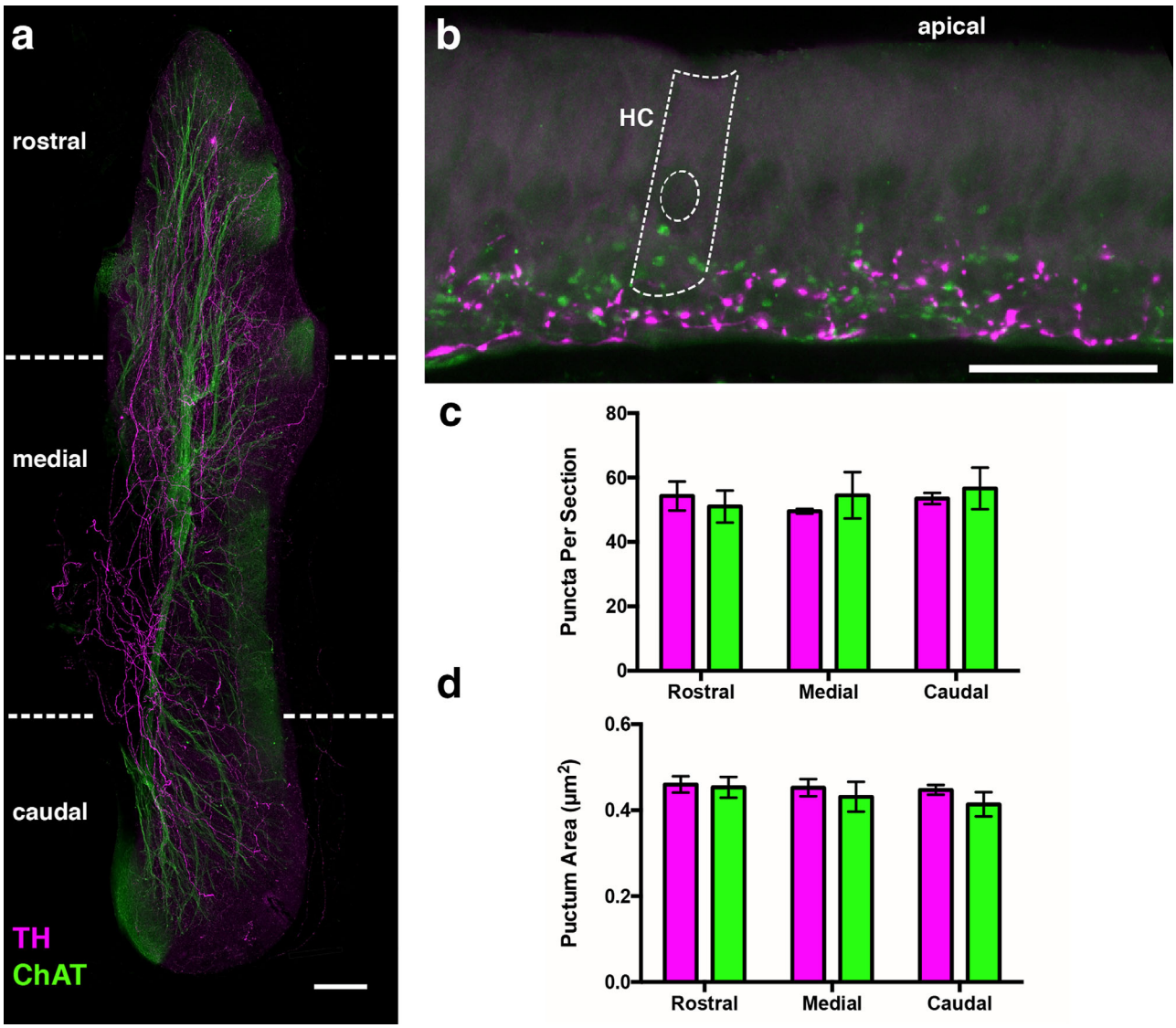

FIGURE 3 Dopaminergic and cholinergic terminals are distributed uniformly across the saccule. (a) Composite confocal micrograph of whole mount saccular epithelium (SE) depicting widespread distribution of tyrosine hydroxylase (TH-ir, purple) and choline-acetyltransferase immunoreactive (ChAT-ir, green) fibers. (b) Representative sagittal section through SE used for analysis. Hair cell (HC) somata are visible as light background. Dotted lines trace the approximate position of an example hair cell somata. Stereocillia of HCs (not labeled) are aligned along apical edge of SE. Note concentration of efferent putative puncta around base of HCs. Quantification of TH-ir and ChAT-ir putative puncta number (c) and size (d) across rostral, medial, and caudal regions of the SE (mean ± standard error). Regions are depicted in (A). Scale bar = 200 μm in (a); 25 μm in (b)

membrane distances of 5–10 nm, are found between support cells (SCs) along the basal edge of the epithelium (Figure 5a, inset).

3.5 | TH-ir profiles in the saccule

TH-ir profiles are found near the basal membrane, in association with SCs and neural processes (Figure 5a). Many profiles have small diameters (80–290 nm) and are likely cross sections of fibers of passage, continuing to the synaptic region around hair cells; however, some profiles have larger diameters (400–550 nm) and contain synaptic vesicles, 28–35 nm in diameter. The DAB-reaction product typically fills the cytoplasm of the entire profile, but remains absent in vesicles and mitochondria. Vesiculated profiles are more commonly observed within 10 μm of the hair cell base, in proximity to afferent-hair cell, efferent-hair cell and efferent–afferent synapses (Figure 5b–d). As can be seen in fluorescent micrographs (Figure 1b), TH-ir fibers form swellings along their length. TH-ir processes sectioned through the longitudinal axis show thin 50–80 nm diameter fibers that swell to a diameter of 400–450 nm and contain vesicles (Figure 6a–f). Unlike afferent and cholinergic efferent profiles, these swellings do not appear to make synaptic contact with other structures. Throughout 45 randomly selected profiles (5 each from rostral, medial and caudal regions of the saccule from 3 animals), serial sections (9–20) did not reveal any synaptic specializations, such as darkening of the postsynaptic membrane (Figure 7a–i).

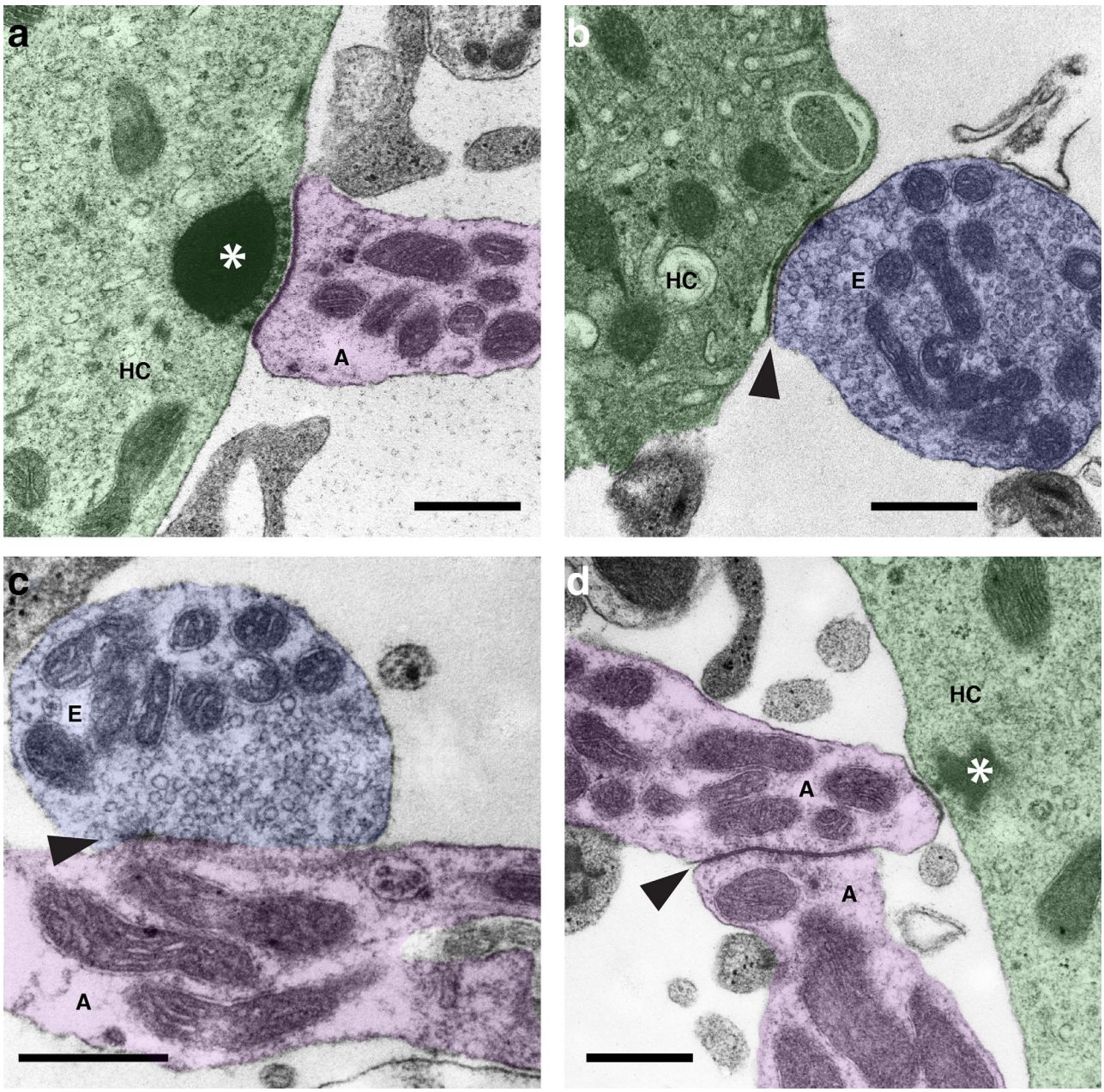

FIGURE 4 Electron micrographs depicting various synapse types present in the saccular epithelium. (a) Afferent synapse between hair cell (HC, green) and primary afferent dendrite (A, purple), which typically contains a presynaptic ribbon (white asterisk, an electron dense spherical object), as well as a postsynaptic density. (b) Efferent synapse (E, blue) at base of a hair cell (HC, green), likely emanating from the cholinergic octavolateralis efferent nucleus (OE). Many synaptic vesicles are present in the presynaptic region while a darkening of the postsynaptic membrane overlays a clear intracellular envelope, the subsynaptic cistern (black arrowhead). (c) Efferent synapse (E, blue) on afferent process (A, purple). Although less common than efferent-hair cell synapses, these were found across all subjects. (d) A tight junctional association (black arrowhead) between two afferent dendrites (A, purple), possibly a gap junction, near an afferent synapse on a hair cell (white asterisk). Synaptic elements depicted in electron micrographs are pseudo-colored for clarity. Scale bar = 500 nm in (a–d) [Color figure can be viewed at wileyonlinelibrary.com]

3.6 | TH-ir profiles in the octavolateralis efferent nucleus

The cells of the OE can be easily identified based on their anatomical location and morphology in semithin and ultrathin sections (compare Figures 1c and 8a). At low magnification, OE somata are surrounded by numerous TH-ir profiles, which appear to directly contact the membrane (Figure 8b). Examination at higher magnification revealed two types of profiles. Some profiles do indeed directly contact the OE somatic membrane, contain synaptic vesicles (28–62 nm) and appear to exhibit symmetric-like synaptic specializations (Figure 8c,i). Another class of TH-ir profile, containing vesicles of similar size, directly abuts unstained axon terminals making direct synapses on OE somata (Figure 8d–h). These unstained terminals are symmetric-like, but vary

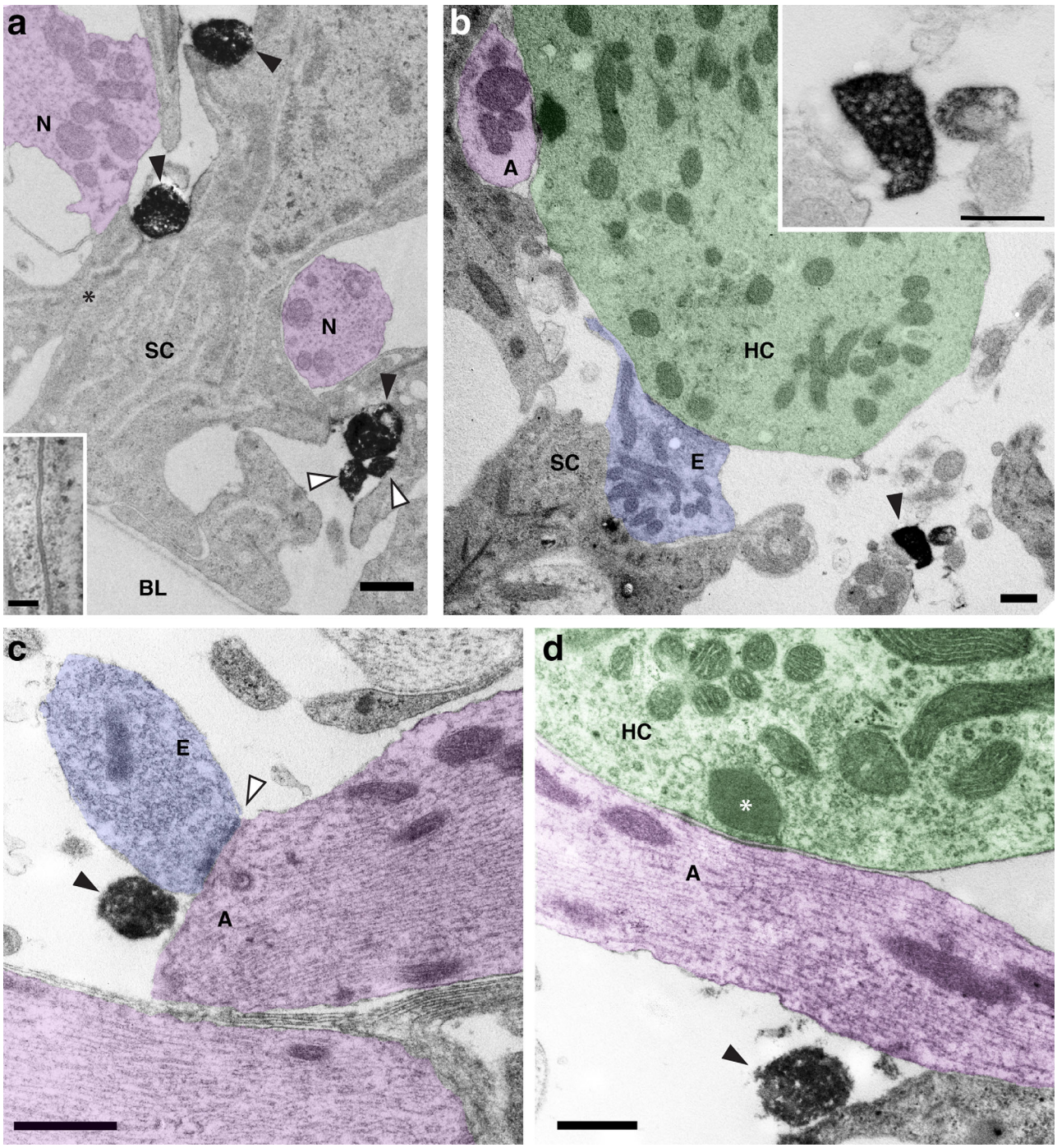

FIGURE 5 Tyrosine hydroxylase immunoreactive (TH-ir) profiles in the saccular epithelium contain synaptic vesicles and are situated near multiple synapse types and junctions. (a) TH-ir profiles near the basal lamina (BL), in association with support cells (SCs) and nerve processes (N, purple), both afferent and efferent. Many profiles are small and likely cross sections of fibers of passage (white arrowheads) continuing to the base of hair cells, however some profiles are larger and appear to contain vesicles (black arrowheads) and are situated near gap junctions between SCs (black asterisk). Inset depicts gap junction. (b) TH-ir profile, containing electron dense reaction product (black arrowhead), near the base of a hair cell (HC, green) with both an efferent (E, blue) and afferent (A, purple) synapse in close proximity. Inset shows vesiculated nature of TH-ir profile. (c) TH-ir profile (black arrowhead) near efferent synapse (E, blue) on an afferent fiber (white arrowhead). (d) Vesiculated TH-ir profile (black arrowhead) in proximity to an afferent fiber (A, purple) making a synapse en passant (white asterisk) with a hair cell (HC, green). Electron micrographs are pseudo-colored for clarity. Scale bar = 500 nm in (a-d); 100 nm for inset of (b) [Color figure can be viewed at wileyonlinelibrary.com]

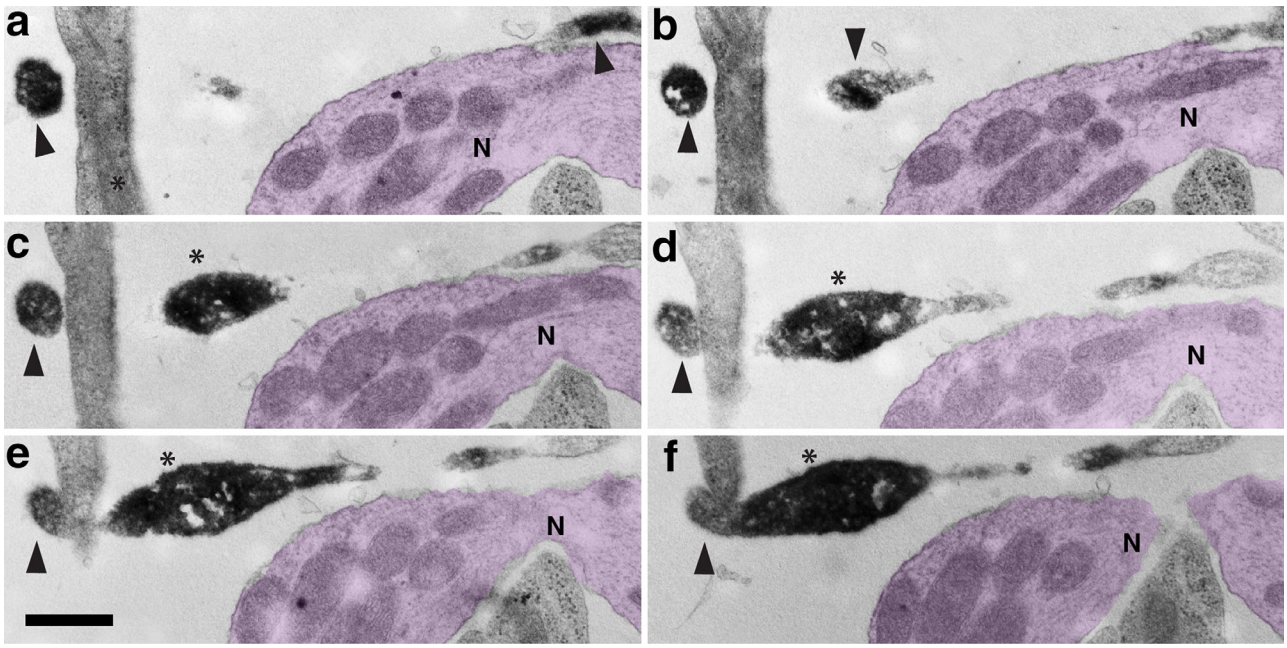

FIGURE 6 Serial sections (a–f) showing a tyrosine hydroxylase immunoreactive profile (black arrowheads and asterisks) as it tracks along a neural process (N, purple) below a hair cell. Diameter of profile varies from 50nm to 400 nm. Note vesiculated appearance of profile where it widens (black asterisks, d–f). Electron micrographs are pseudo-colored for clarity. Scale bar = 500 nm in (a–f) [Color figure can be viewed at wileyonlinelibrary.com]

in their vesicle morphology, with either pleomorphic (30–36 nm) or round synaptic vesicles (27–33 nm). Unstained asymmetric-like synapses are occasionally observed on OE somata, but always without abutting TH-ir profiles (Figure 8j). OE neurons have large ventro-lateral projecting dendrites (OEds) that are tracked by prominent TH-ir fibers (Figures 1c and 9a). OEds can be readily identified and followed in semithin and serial ultrathin sections for 50-150 μm from OE neurons (Figure 9b). OEd-contacting TH-ir profiles are similar in appearance to direct contacts on OE somata, with small synaptic vesicles (29–56 nm), but with either symmetric-like or asymmetric-like synaptic specializations (Figure 9c–g). While TH-ir profiles were not found to form synapses with unlabeled terminals on OEds, we did observe profiles in the surrounding neuropil, in association with unidentified processes, not more than 10 μm from identified OEds (Figure 9h–j).

4 | DISCUSSION

Our combined tract tracing, immunohistochemical and electron microscopy results extend our previous findings (Forlano et al., 2014, Forlano, Ghahramani et al., 2015) further supporting DA as a modulator of both the inner ear and the hindbrain auditory efferent system.

4.1 | Catecholaminergic innervation of the auditory periphery and efferent nucleus is dopaminergic

The localization of TH-ir to profiles containing synaptic vesicles in the saccule and OE supports release of catecholamines (CA), which include DA and NA. The centrifugal CA innervation of the saccule is exclusively dopaminergic, as the only TH-ir neurons identified via tract tracing from the saccule reside in the dopaminergic TPp in the diencephalon (Forlano et al., 2014) and we observed no DBH-ir signal in the saccular epithelium. The lack of DBH co-localization with TH fibers indicates that CA input to the OE is also dopaminergic. The OE of teleosts has widespread projections to all mechanosensory endorgans and is considered to represent the plesiomorphic (ancestral) state of the vertebrate auditory efferent system (Fritzsch, 1999; Köppl, 2011; Simmons, 2002). In the derived efferent system of mammals, anatomically distinct subpopulations of efferent neurons in the hindbrain project exclusively to either the cochlea or vestibular endorgans. Several studies have documented noradrenergic and serotonergic input to cochlear efferent neurons (Brown, 2011; Mulders & Robertson, 2000, 2005; Thompson & Thompson, 1995; Woods & Azeredo, 1999). Interestingly, we also observe serotonergic fibers making putative contacts on OE neurons of midshipman (Timothy and Forlano, unpublished observations). In contrast, DA innervation of cochlear efferent neurons has only been investigated in a single study, in guinea pig, where the authors concluded that based upon the absence of DA antibody labeling, putative TH-ir contacts on efferent neurons are all noradrenergic (Mulders & Robertson, 2005). However, a more recent study in mice shows projections throughout the auditory brainstem originating from dopaminergic A11 neurons in the subparafascicular thalamic nucleus (Nevue, Felix, & Portfors, 2016), though they did not confirm DA contacts on cochlear efferent neurons. In general, additional studies of DA innervation of auditory efferents are needed in mammals as well as other anamniotes. It is therefore an open question as to whether direct DA modulation of the auditory efferent system is an ancestral feature that has been universally lost in mammals or is a more recently derived and unique adaptation in fishes.

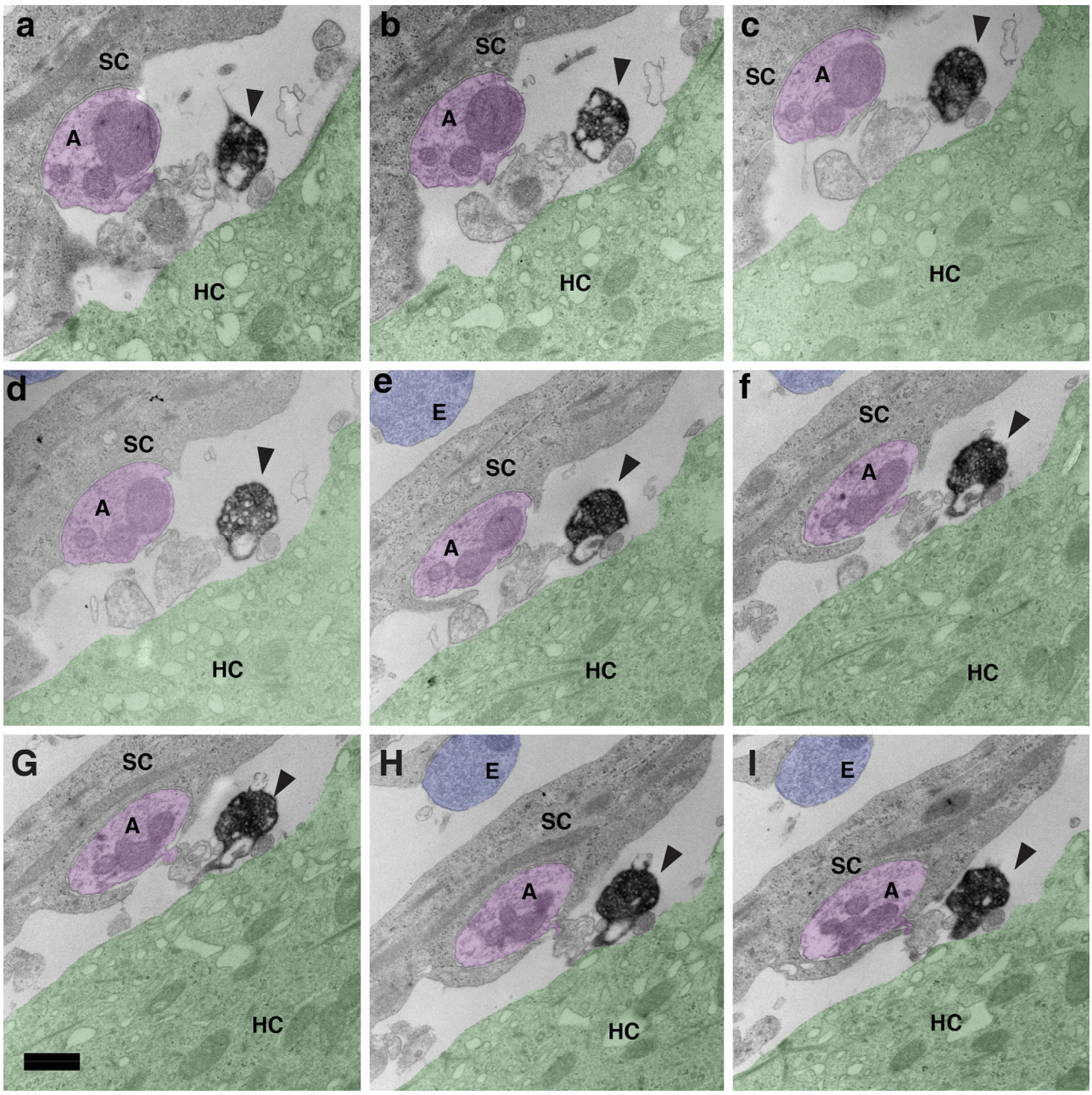

FIGURE 7 Tyrosine hydroxylase immunoreactive (TH-ir) profiles do not form traditional synapses in the saccular epithelium. Serial sections (a–i) show a vesiculated TH-ir profile (black arrowhead) adjacent to a hair cell (HC, green) and afferent process (A, purple) cradled by a support cell (SC). No synaptic specializations were observed. Efferent bouton (E) is blue. Electron micrographs are pseudo-colored for clarity. Scale bar = 500 nm in (a–i) [Color figure can be viewed at wileyonlinelibrary.com]

The TPp was the only CA nucleus rostral to the OE with backfilled cells. Area postrema (AP) and the vagal lobe (XL) contain a mix of NA and DA cells (Kaslin & Panula, 2001; Ma, 1997) and while we cannot rule out a dopaminergic contribution to the OE from these cell groups, they are likely to be minimal for the following reasons: (a) TH-ir fiber projections examined in multiple planes of section appear to originate from descending CA tracts (Forlano et al., 2014) and (b) a projectome study in larval zebrafish showed that CA neurons in AP have mostly local or diencephalic targets and XL-associated CA neurons have mostly local projections (Tay et al., 2011). The connectivity of the TPp has been most thoroughly investigated in larval zebrafish, where *individual* DA neurons have extensive ascending and descending axonal arborizations and innervate multiple targets, including spinal cord and lateral line neuromasts (Jay, De Faveri, & McDearmid, 2015; Tay et al., 2011). In mice, individual DA neurons from the A11 group project to both the inferior colliculus and the auditory brainstem (Nevue et al., 2016). Importantly, the TPp is a proposed homolog of the mammalian A11 group of DA neurons (Schweitzer et al., 2012; Yamamoto & Vernier, 2011). It is possible that in midshipman, the same dopaminergic TPp neurons that innervate the saccular epithelium also project to the OE. Regardless, the connectivity we have demonstrated here, along with our previous work showing that the TPp also contributes dopaminergic input to other

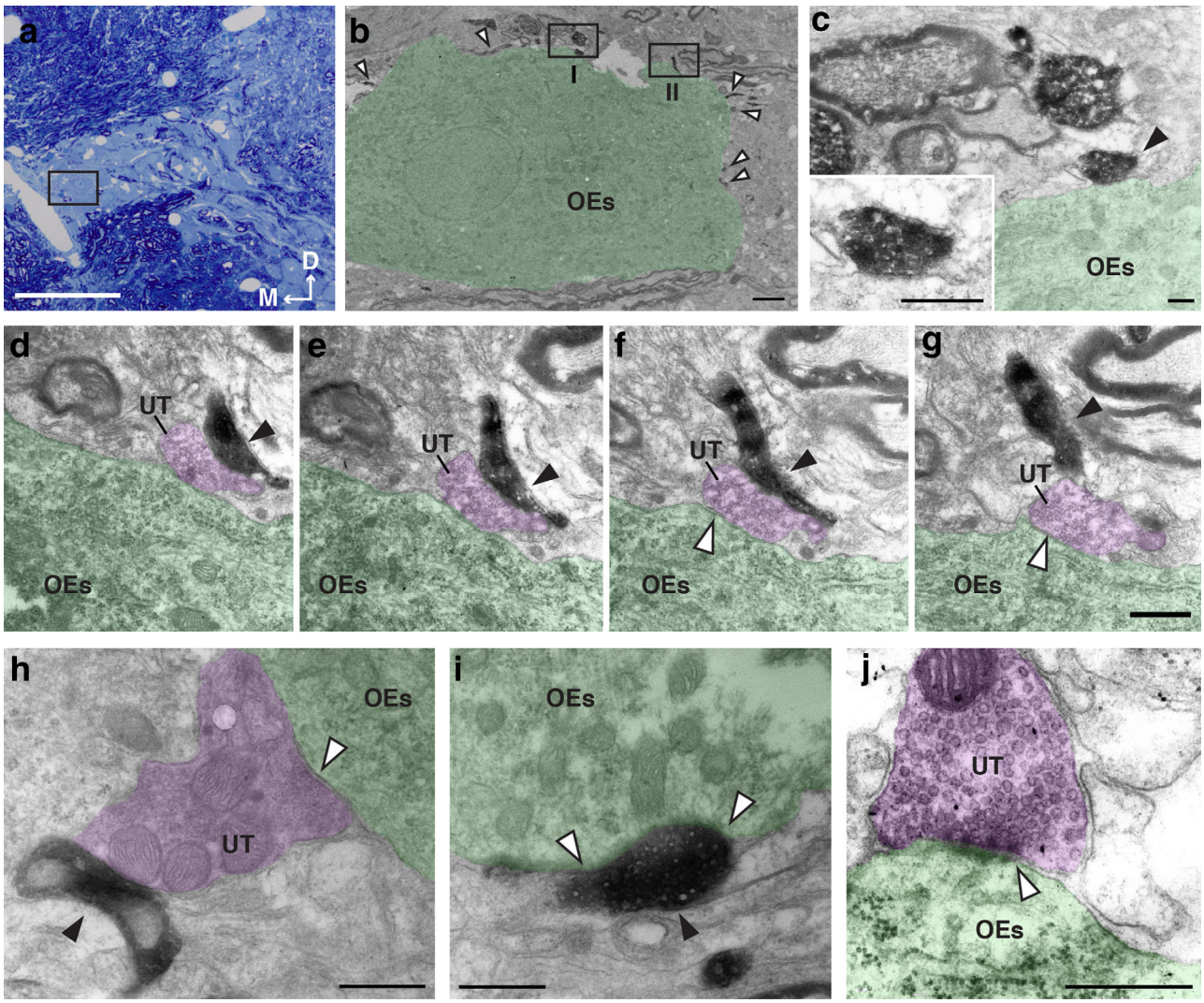

FIGURE 8 Tyrosine hydroxylase immunoreactive (TH-ir) profiles make direct and indirect contacts with octavolateralis efferent (OE) neurons. (a) Light micrograph depicts 0.5 μm thick transverse section containing OE neurons. Cytoarchitecture visualized with methylene blue. White arrows indicate medial (M) and dorsal (D) orientation. Box highlights soma shown in (b), taken from subsequent serial section. (b) Low mag electron micrograph shows OE soma (OEs, green) surrounded by numerous TH-ir profiles (white arrowheads). (c) Higher magnification of TH-ir profile (black arrowhead) from box I in (b). Inset shows magnified image of profile. Note direct apposition to soma membrane and vesiculated appearance. (d–g) Serial sections through a TH-ir profile (black arrowhead, box II in b) abutting an unlabeled axon terminal (UT, purple) on OEs (green). Note both vesiculated appearance of TH-ir profile (most apparent in e) as well as symmetric synapse of unlabeled axon terminal (white arrowheads in f, g). Additional examples of (h) indirect TH-ir profile (black arrowhead) contacting unlabeled symmetric axon terminal (UT, purple) synapsing (white arrowhead) on OEs and (i) large vesiculated TH-ir swelling (black arrowhead) directly contacting OEs (white arrowheads). (j) Unstained axon terminal (UT, purple) forming an asymmetric synapse (white arrowhead) with OEs. TH-ir profiles were never found in contact with these terminal types. Electron micrographs are pseudo-colored for clarity. Scale bar = 100 μm in (a); 2 μm in (b); 100nm in (c); 500 nm for inset in (c), and (d–j) [Color figure can be viewed at wileyonlinelibrary.com]

vocal-acoustic circuitry (Forlano et al., 2014), suggests an integrative role for DA TPp neurons in auditory-driven social behaviors.

4.2 | Synaptology and efferent input to the saccule of the inner ear

Unlike the mechanically tuned mammalian cochlea, the saccules of some fishes possess a crude tonotopic organization (Fay, 1978; Furukawa & Ishii, 1967; Sisneros, 2007) that has been suggested to arise from regional variation of hair cell morphology or efferent innervation (Popper & Fay, 1999; Popper & Saidel, 1990). Regional efferent modulation in the saccule has also been proposed as a mechanism to support sound source localization (Edds-Walton, Fay, & Highstein, 1999). Our confocal analysis did not reveal any regional differences in TH-ir or ChAT-ir putative puncta, suggesting that regional differences in thresholds are not attributable to efferent innervation patterns.

The fine structure of the midshipman saccule is comparable to that of the closely related oyster toadfish (Sokolowski & Popper, 1988) and other fishes (Hama, 1969; Jenkins, 1979; Popper & Fay, 1999; Wegner, 1982). Gap junctions between SCs have been widely reported and

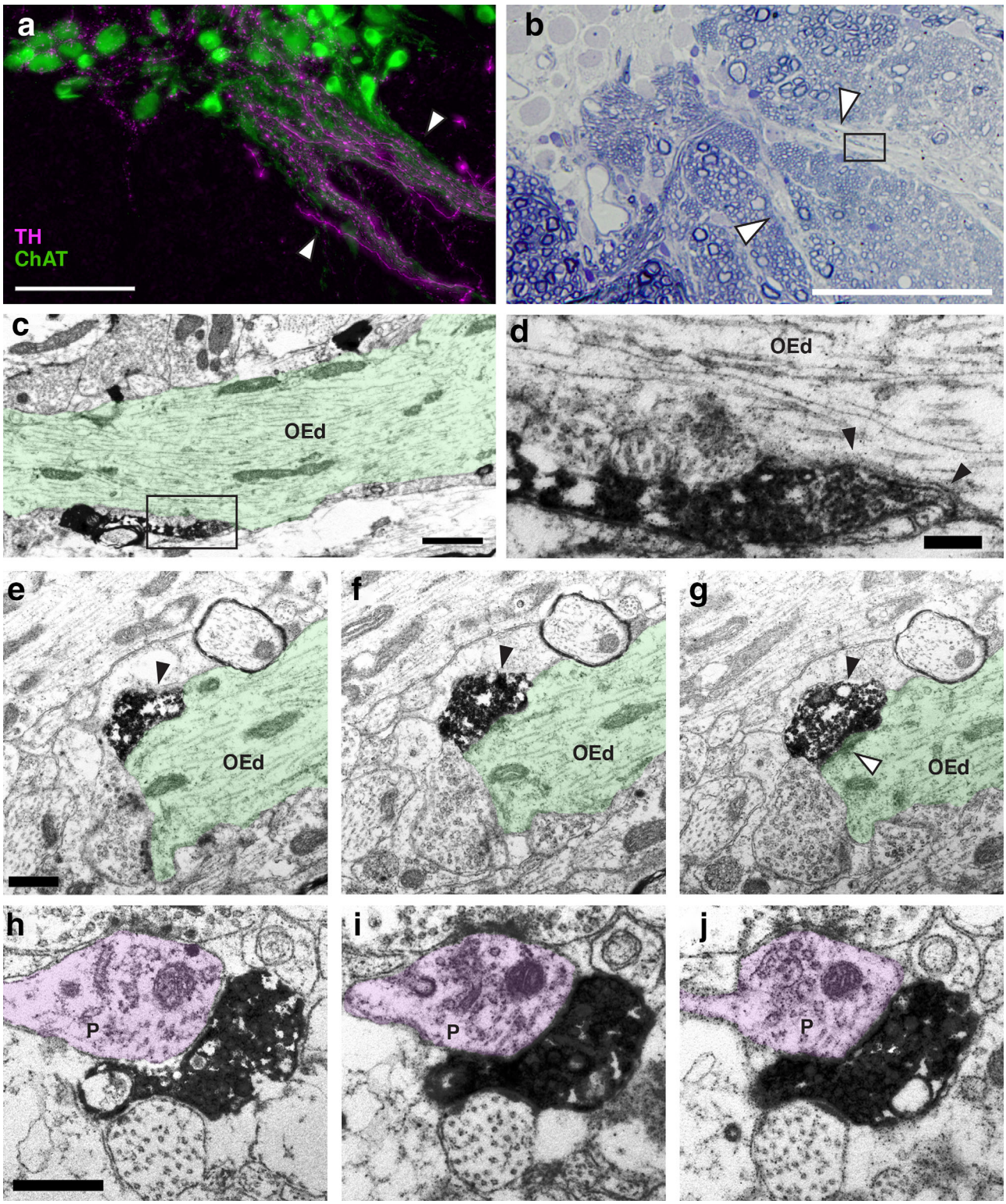

FIGURE 9 Tyrosine hydroxylase immunoreactive (TH-ir) profiles form direct contacts with proximal octavolateralis efferent (OE) dendrites. (a) Fluorescent micrograph showing robust varicose TH-ir fibers (purple, white arrowheads) tracking along cholinergic fibers (ChAT-ir, green) emanating from OE neurons. (b) Light micrograph showing OE fibers (white arrowheads) in semithin section at similar scale and location to (a). Cytoarchitecture visualized with methylene blue. Box indicates area shown in c from subsequent section. (c) TH-ir neurite tracks and forms a direct contact (box) with OE dendrite (OEd). (d) High mag micrograph of TH-ir profile from (c). Note vesicles and direct, symmetric synapse with OEd (black arrowheads). (e–g) Consecutive serial sections depicting vesiculated TH-ir profiles (black arrowheads) forming asymmetric-like synapse on OEd (white arrowhead). (h–j) Consecutive serial sections depicting vesiculated TH-ir contact on unlabeled profile (P, purple) in the neuropil surrounding OEds. Electron micrographs are pseudo-colored for clarity. Scale bar = 50 μm in (a, b); 1 μm in (c); 200 nm in (d); 500 nm in (e–j) [Color figure can be viewed at wileyonlinelibrary.com]

confirmed with freeze-fracture EM (Hama, 1980; Hama & Saito, 1977; Wegner, 1982). Afferent and efferent synapses with hair cells can be easily identified based upon their morphology. The efferent-hair cell synapses we describe have been previously identified as cholinergic using both light and electron microscopy (Forlano, Ghahramani et al., 2015; Khan, Hatfield, Drescher, & Drescher, 1991; Sugihara, 2001) and have an inhibitory effect on hair cells (Furukawa, 1981; Katz, Elgoyhen, & Fuchs, 2011).

We also report efferent varicosities synapsing directly onto afferent processes. Although less common in comparison to efferent-hair cell synapses, where a hair cell can been seen to receive 1–3 efferent terminals in a single thin section, such efferent–afferent synapses are consistently seen across subjects in this study and have also been described in goldfish saccule and semicircular canal (Lanford & Popper, 1996; Nakajima & Wang, 1974), oyster toadfish utricle and semicircular canal (Sans & Highstein, 1984), sea eel lateral line (Hama, 1978), and rainbow trout saccule, utricle and semicircular canal (Khan et al., 1991, Khan, Drescher, Hatfield, & Drescher, 1993). Indeed, this synapse type is conserved across vertebrates (Köppl, 2011). Like efferent-hair cell synapses, these junctions appear to be cholinergic, as verified in trout saccule by histochemical localization of acetylcholinesterase (Khan et al., 1991). Interestingly, efferent–afferent synapses may exert an excitatory modulatory action, in contrast to inhibitory efferent-hair cell synapses, although this has only been examined in vestibular afferents (Boyle, Rabbitt, & Highstein, 2009). Perhaps owning to their rarity, the distribution and function of this synapse type has not been systemically investigated in teleost hearing endorgans.

The membrane specializations between afferent processes we describe have only, to our knowledge, previously been reported in oyster toadfish, where it is suggested that they are gap junctions (Sokolowski & Popper, 1988). The distances we observed between afferent membranes in the present study, 8–12 nm, is similar to the distances between membranes at support cell gap junctions, 5–10 nm, which are found in numerous vertebrates (Forge et al., 2003; Hama, 1980). The confirmation of gap junctions between afferent neuronal processes will require further investigation with freeze-fracture analysis or immunohistochemistry.

4.3 | Evidence for volumetric release of dopamine in the inner ear

The asynaptic quality of dopaminergic terminals in the midshipman saccule is a novel, though not unexpected observation, since CA systems are known to utilize volumetric release from varicosities lacking traditional synaptic contacts (Descarries & Mechawar, 2000; Pickel, Nirenberg, & Milner, 1996). Ultrastructural evidence for dopaminergic volume transmission in teleosts has been reported in the retina, pituitary, and hindbrain (Pereda, Triller, Korn, & Faber, 1992; Peute et al., 1987; Yazulla & Studholme, 1995). Previous ultrastructure investigations of dopaminergic innervation of hearing endorgans are limited to guinea pig cochlea, where profiles immunoreactive for TH and aromatic amino acid decarboxylase (the enzyme that converts L-DOPA to DA) directly abut afferent and unstained efferent fibers and inner hair cells in the organ of Corti; however, only contacts with afferents display traditional synaptic structures (d'Aldin et al., 1995; Eybalin et al., 1993). These studies did not systematically examine serial sections so it is unclear whether all DA varicosities form synapses, or only a subset. Using confocal microscopy, a partial mismatch was reported between dopaminergic puncta and receptors in the immature mouse cochlea, where D1-like and D2-like receptors are localized to regions of the auditory afferent fibers that are up to 15 μm away from putative DA release sites, suggesting diffuse transmission (Maison et al., 2012). Similarly, confocal microscopy was used to show that putative dopaminergic terminals do not colocalize with D1-like receptors on hair cells in larval zebrafish lateral line neuromasts (Toro et al., 2015).

Paracrine release of DA could affect multiple targets in the saccule. The location of vesiculated TH-ir profiles close to the basal membrane of the saccular epithelium, where afferent nerve fibers first become myelinated (Saidel, Popper, & Chang, 1990), may facilitate modulation of afferent neurons near the site of action potential initiation, as proposed in mammals (Maison et al., 2012). DA may also act upon midshipman hair cells or could modulate the cholinergic action of efferents on hair cells or afferents. Physiological studies in rodents are somewhat paradoxical, but mostly describe an inhibitory effect of DA on cochlear afferent neurons with no effect on direct measures of inner hair cell function (d'Aldin et al., 1995; Lendvai et al., 2011; Ruel et al., 2001; Sun & Salvi, 2001; Valdés-Baizabal, Soto, & Vega, 2015), but some evidence for direct modulation of outer hair cells (Garrett, Robertson, Sellick, & Mulders, 2011; Maison et al., 2012). Although functional studies are lacking in nonmammalian hearing organs, DA has an inhibitory effect on both the VIII nerve in larval zebrafish (Mu, Li, Zhang, & Du, 2012) and the afferent nerve in the frog semicircular canal, which serves a singularly vestibular function (Andrianov, Ryzhova, & Tobias, 2009). In contrast, DA increases the excitability of hair cells in the zebrafish lateral line through a D1-like receptor mechanism (Toro et al., 2015). Isolated hair cells from rainbow trout express both D1-like and D2-like receptor mRNA (Drescher et al., 2010), as do homogenates of larval zebrafish utricular and saccular maculae (Toro et al., 2015). To our knowledge, there is no evidence for a direct DA modulation of cholinergic efferents in the peripheral auditory system, but dopaminergic and cholinergic systems have well characterized interactions in the central nervous system (Acquas & Chiara, 2002; Moore, Fadel, Sarter, & Bruno, 1999). Another possibility, as suggested by basally located vesiculated TH-ir profiles, is that DA may interact with the gap junctions between SCs. In the teleost retina, DA gates gap junction permeability, reducing their open state probability (McMahon, Knapp, & Dowling, 1989). The network of gap junctions between SCs is thought to be important for regulating the ionic concentration of both the perilymph, which surrounds the hair cells and associated neural processes, and endolymph, which bathes the apical surface of hair cells, and which could influence multiple aspects of hair cell physiology, including frequency tuning or thresholds (Chang-Chien et al., 2014; Ghanem, Breneman, Rabbitt, & Brown, 2008; Zhu et al., 2013). Interestingly, DA appears to alter ion exchange activity in SCs of the stria vascularis of the guinea pig cochlea (Kanoh, 1995).

4.4 | Dopaminergic input to hindbrain auditory efferents shows synaptic heterogeneity

The heterogeneous mixture of synaptic terminal types in the OE suggests numerous mechanisms through which the dopaminergic TPp could modulate the cholinergic auditory efferent system. TH-ir synapses on OE somata and dendrites strongly support direct DA modulation of OE neurons. The symmetric synaptic specializations and transmitter vesicle morphology of unlabeled, TH-ir-profile contacted terminals are characteristic of inhibitory synapses containing GABA or glycine (Helfert et al., 1992; Peters & Palay, 1996). Thus, DA innervation may also indirectly modulate somatic inhibition. In contrast to direct contacts on somata, which were symmetric-like, TH-ir synapses on proximal OE dendrites exhibited both symmetric-like and asymmetric-like synapses. Unlike glutamatergic and GABAergic synapses, the fine structure of CA synapses cannot be reliably correlated with their modulatory function (Pickel et al., 1996). Recent evidence from larval zebrafish shows that dopaminergic TPp neurons express vesicular glutamate transporter-2 mRNA (Filippi, Mueller, & Driever, 2014), suggesting that the TH-ir asymmetric synapses we observed on OE dendrites may co-release glutamate. There is disagreement in the literature concerning whether DA and glutamate are released from the same or segregated axon terminals (Descarries et al., 2008; Hnasko et al., 2010; Zhang et al., 2015), so elucidating co-transmission in the OE will require further ultrastructure studies that employ antibody markers for both DA and glutamate transporters or receptors.

There are two pathways through which TPp axons could innervate the OE: (a) a descending medial efferent bundle that appears to first target OE somata and continue on the dendritic field and (b) a more laterally situated descending medial longitudinal catecholaminergic tract that appears to first target the OE dendritic field (Forlano et al., 2014). While both of these pathways could contribute equally to the range of DA inputs to OE somata and dendrites, it is possible that the different DA synapse types we observed could share distinct pathways. For example, direct DA contacts on somata might arise from the medial efferent bundle and indirect DA contacts on the unlabeled inhibitory-like terminals might arise from the medial longitudinal tract. This would suggest functionally and anatomically distinct subdivisions of the TPp, a possibility that could be investigated by filling individual TPp neurons and identifying their synaptic terminals throughout the OE.

We were unable to discern the identity of unlabeled profiles that received TH-ir contacts in the neuropil surrounding OE dendrites. While these may be finer processes either emanating from or contacting OE dendrites, we did not observe connections between the unlabeled profiles and OE dendrites in serial sections. DA contacts on these structures are therefore unlikely to contribute to modulation of the OE.

4.5 | Functional implications of direct and indirect dopaminergic modulation of the auditory periphery

Our observations raise intriguing questions concerning seasonal changes in DA innervation in the saccule and OE. Using fluorescent microscopy, we demonstrated that DA innervation is reduced in the saccule and greater in the OE in females during the summer breeding versus the winter nonreproductive season (Forlano, Ghahramani et al., 2015). Taken together with the well-documented enhancement of hearing sensitivity in the summer, this suggested an inhibitory effect of DA in both the saccule and the OE (Forlano & Sisneros, 2016; Forlano, Sisneros et al., 2015). A reduction of DA in the saccule would decrease direct inhibition of peripheral auditory processing, and an increase of DA in the OE would result in a reduction of the inhibitory drive of cholinergic efferents to the saccule. A summer decrease in the number and size of vesiculated TH-ir profiles in the saccule would be consistent with our light microscopy observations and the proposed inhibitory function of DA in the periphery. Seasonal synaptic differences could be more complex in the OE. If DA inhibits OE neurons, we would predict a summer increase in direct TH-ir contacts on OE somata and dendrites, but a decrease in TH-ir contacts on unlabeled, inhibitory-like terminals on OE somata. However, if DA excites OE neurons, we would expect the opposite pattern, consistent with a reduction of cholinergic inhibition in the saccule. If the asymmetric-like DA terminals are glutamatergic and excitatory, we would predict a summer reduction in these terminals. There is evidence for both D1-like and D2-like receptor mRNA expression in OE neurons in the European eel (Kapsimali, Vidal, González, Dufour, & Vernier, 2000; Pasqualini et al., 2009). If DA receptor expression is similarly diverse in the midshipman OE, then localization of receptor subtypes in somata and dendrites may clarify the modulatory function of DA and the downstream effects of seasonal variation of innervation. Future quantitative studies will test these hypotheses and may reveal important seasonal changes in dopaminergic ultrastructure and receptor expression that contribute to auditory plasticity in midshipman (Forlano, Ghahramani, et al., 2015; Forlano & Sisneros, 2016).

The present study is the first to examine the ultrastructure of DA innervation in both the inner ear and hindbrain auditory efferent system in a nonmammalian vertebrate. While the implications of this work to the evolution of the auditory efferent system will require further insights from other anamniotes, the well-characterized vocal courtship behaviors of the midshipman along with the accessibility of its auditory system should be a profitable model in which to uncover the biological function of DA in the inner ear and its role in acoustic communication.

ACKNOWLEDGMENTS

We wish to thank Renee M. May for TEM technical advice and Spencer D. Kim for assistance with tissue preparation.

CONFLICT OF INTEREST

The authors declare no known or potential conflicts of interest.

AUTHOR CONTRIBUTION

All authors had full access to all the data in the study and take responsibility for the integrity of the data and the accuracy of the data analysis. Study concept and design: PMF and JTP. Acquisition of data: PMF and JTP. Analysis and interpretation of data: PMF and JTP. Drafting of the manuscript: JTP. Critical revision of the

manuscript for important intellectual content: PMF. Obtained funding: PMF and JTP.

REFERENCES

Acquas, E., & Chiara, G. D. (2002). Dopamine-acetylcholine interactions. In G. D. Chiara (Ed.), *Dopamine in the CNS II* (pp. 85–115). Berlin: Springer.

Adrio, F., Anadón, R., & Rodríguez-Moldes, I. (2000). Distribution of choline acetyltransferase (ChAT) immunoreactivity in the central nervous system of a chondrostean, the Siberian sturgeon (*Acipenser baeri*). *The Journal of Comparative Neurology*, *426*, 602–621.

Adrio, F., Anadón, R., & Rodríguez-Moldes, I. (2002). Distribution of tyrosine hydroxylase (TH) and dopamine beta-hydroxylase (DBH) immunoreactivity in the central nervous system of two chondrostean fishes (Acipenser baeri and Huso huso). *The Journal of Comparative Neurology*, *448*, 280–297.

Anadón, R., Molist, P., Rodríguez-Moldes, I., López, J. M., Quintela, I., Cerviño, M. C., … González, A. (2000). Distribution of choline acetyltransferase immunoreactivity in the brain of an elasmobranch, the lesser spotted dogfish (*Scyliorhinus canicula*). *The Journal of Comparative Neurology*, *420*, 139–170.

Andéol, G., Guillaume, A., Micheyl, C., Savel, S., Pellieux, L., & Moulin, A. (2011). Auditory efferents facilitate sound localization in noise in humans. *The Journal of Neuroscience: The Official Journal of the Society for Neuroscience*, *31* 6759–6763.

Andrianov, G. N., Ryzhova, I. V., & Tobias, T. V. (2009). Dopaminergic modulation of afferent synaptic transmission in the semicircular canals of frogs. *Neurosignals*, *17*, 222–228.

Bass, A. H. (1996). Shaping brain sexuality. *American Scientist*, *84*, 352–363.

Bass, A. H., Bodnar, D. A., & Marchaterre, M. A. (2000). Midbrain acoustic circuitry in a vocalizing fish. *The Journal of Comparative Neurology*, *419*, 505–531.

Bass, A. H., & Clark, C. W. (2003). The physical acoustics of underwater sound communication. In A. M. Simmons, R. R. Fay, & A. N. Popper (Eds.), *Acoustic communication* (pp. 15–64). New York: Springer.

Bass, A. H., Marchaterre, M. A., & Baker, R. (1994). Vocal-acoustic pathways in a teleost fish. *The Journal of Neuroscience: The Official Journal of the Society for Neuroscience*, *14*, 4025–4039.

Belfry, C. S., & Cowan, F. B. M. (1995). Peptidergic and adrenergic innervation of the lachrymal gland in the euryhaline turtle, *Malaclemys terrapin*. *The Journal of Experimental Zoology*, *273*, 363–375.

Bhandiwad, A. A., Whitchurch, E. A., Colleye, O., Zeddies, D. G., Sisneros, J. A. (2017). Seasonal plasticity of auditory saccular sensitivity in "sneaker" type II male plainfin midshipman fish, Porichthys notatus. *Journal Comparative Physiology A*, *203*, 211–222.

Boyle, R., Rabbitt, R. D., & Highstein, S. M. (2009). Efferent control of hair cell and afferent responses in the semicircular canals. *Journal of Neurophysiology*, *102*, 1513–1525.

Brantley, R. K., & Bass, A. H. (1988). Cholinergic neurons in the brain of a teleost fish (*Porichthys notatus*) located with a monoclonal antibody to choline acetyltransferase. *The Journal of Comparative Neurology*, *275*, 87–105.

Brantley, R. K., & Bass, A. H. (1994). Alternative male spawning tactics and acoustic signals in the plainfin midshipman fish *Porichthys notatus* Girard (Teleostei, Batrachoididae). *Ethology*, *96*, 213–232.

Brown, M. C. (2011). Anatomy of olivocochlear neurons. In D. K. Ryugo, R. R. Fay, & A. N. Popper (Eds.), *Auditory and vestibular efferents* (pp. 17–37). New York: Springer.

Bullman, T., Hartig, W., Holzer, M., & Arendt, T. (2010). Expression of the embryonal isoform (0N/3R) of the microtuble-associated protein tau in the adult rat central nervous system. *The Journal of Comparative Neurology*, *518*, 2538–2553.

Castelino, C. B. & Ball, G. F. (2005). A role for norepinephrine in the regulation of context-dependent ZENK expression in male zebra finches (*Taeniopygia guttata*). *The European journal of Neuroscience*, *21*, 1962–1972.

Chagnaud, B. P., & Bass, A. H. (2013). Vocal corollary discharge communicates call duration to vertebrate auditory system. *The Journal of Neuroscience: The Official Journal of the Society for Neuroscience*, *33*, 18775–18780.

Chang-Chien, J., Yen, Y. C., Chien, K. H., Li, S. Y., Hsu, T. C., & Yang, J. J. (2014). The connexin 30.3 of zebrafish homologue of human connexin 26 may play similar role in the inner ear. *Hearing Research*, *313*, 55–66.

Coffin, A. B., Mohr, R. A., & Sisneros, J. A. (2012). Saccular-specific hair cell addition correlates with reproductive state-dependent changes in the auditory saccular sensitivity of a vocal fish. *The Journal of Neuroscience: The Official Journal of the Society for Neuroscience*, *32*, 1366–1376.

Cohen, M. J., & Winn, H. E. (1967). Electrophysiological observations on hearing and sound production in the fish, *Porichthys notatus*. *The Journal of Experimental Zoology*, *165*, 355–369.

d'Aldin, C., Eybalin, M., Puel, J. L., Charachon, G., Ladrech, S., & Pujol, R. (1995). Synaptic connections and putative functions of the dopaminergic innervation of the guinea pig cochlea. *European Archives of Oto-Rhino-Laryngology: Official Journal of the European Federation of Oto-Rhino-Laryngological Societies (EUFOS): Affiliated with the German Society for Oto-Rhino-Laryngology - Head and Neck Surgery*, *252*, 270–274.

Darrow, K. N., Maison, S. F., & Liberman, M. C. (2006). Cochlear efferent feedback balances interaural sensitivity. *Nature Neuroscience*, *9*, 1474–1476.

Darrow, K. N., Simons, E. J., Dodds, L., & Liberman, M. C. (2006). Dopaminergic innervation of the mouse inner ear: Evidence for a separate cytochemical group of cochlear efferent fibers. *The Journal of Comparative Neurology*, *498*, 403–414.

Descarries, L., Bérubé-Carrière, N., Riad, M., Bo, G. D., Mendez, J. A., & Trudeau, L.É. (2008). Glutamate in dopamine neurons: Synaptic versus diffuse transmission. *Brain Research. Brain Research Reviews*, *58*, 290–302.

Descarries, L., & Mechawar, N. (2000). Ultrastructural evidence for diffuse transmission by monoamine and acetylcholine neurons of the central nervous system. *Progress in Brain Research*, *125*, 27-47.

Drescher, M. J., Cho, W. J., Folbe, A. J., Selvakumar, D., Kewson, D. T., Abu-Hamdan, M. D., … Drescher, D. G. (2010). An adenylyl cyclase signaling pathway predicts direct dopaminergic input to vestibular hair cells. *Neuroscience*, *171*, 1054–1074.

Edds-Walton, P. L., Fay, R. R., & Highstein, S. M. (1999). Dendritic arbors and central projections of physiologically characterized auditory fibers from the saccule of the toadfish, *Opsanus tau*. *The Journal of Comparative Neurology*, *411*, 212–238.

Ekström, P., Honkanen, T., & Borg, B. (1992). Development of tyrosine hydroxylase-, dopamine-, and dopamine B-hydroxylase-immunoreactive neurons in a teleost, the three-spined stickleback. *Journal of Chemical Neuroanatomy*, *5*, 481–501.

Eybalin, M., Charachon, G., & Renard, N. (1993). Dopaminergic lateral efferent innervation of the guinea-pig cochlea: Immunoelectron microscopy of catecholamine-synthesizing enzymes and effect of 6-hydroxydopamine. *Neuroscience*, *54*, 133–142.

Fay, R. R. (1978). Coding of information in single auditory-nerve fibers of the goldfish. *The Journal of the Acoustical Society of America*, *63*, 136–146.

Filippi, A., Mueller, T., & Driever, W. (2014). vglut2 and gad expression reveal distinct patterns of dual GABAergic versus glutamatergic cotransmitter phenotypes of dopaminergic and noradrenergic neurons in the zebrafish brain. *The Journal of Comparative Neurology*, *522*, 2019–2037.

Fine, M. L., & Lenhardt, M. L. (1983). Shallow-water propagation of the toadfish mating call. *Comparative Biochemistry and Physiology. A, Comparative Physiology*, *76*, 225–231.

Forge, A., Becker, D., Casalotti, S., Edwards, J., Marziano, N., & Nevill, G. (2003). Gap junctions in the inner ear: Comparison of distribution patterns in different vertebrates and assessement of connexin composition in mammals. *The Journal of Comparative Neurology*, *467*, 207–231.

Forlano, P. M., Ghahramani, Z. N., Monestime, C. M., Kurochkin, P., Chernenko, A., & Milkis, D. (2015). Catecholaminergic innervation of central and peripheral auditory circuitry varies with reproductive state in female midshipman fish, *Porichthys notatus*. *PLoS One*, *10*, e0121914.

Forlano, P. M., Kim, S. D., Krzyminska, Z. M., & Sisneros, J. A. (2014). Catecholaminergic connectivity to the inner ear, central auditory, and vocal motor circuitry in the plainfin midshipman fish *Porichthys notatus*. *The Journal of Comparative Neurology*, *522*, 2887–2927.

Forlano, P. M., Maruska, K. P., Sisneros, J. A., & Bass, A. H. (2016). Hormone-dependent plasticity of auditory systems in fishes. In A. H. Bass, J. A. Sisneros, A. N. Popper, & R. R. Fay (Eds.), *Hearing and hormones* (pp. 15–51). New York: Springer.

Forlano, P. M., & Sisneros, J. A. (2016). Neuroanatomical evidence for catecholamines as modulators of audition and acoustic behavior in a vocal teleost. In J. A. Sisneros (Ed.), *Fish hearing and bioacoustics* (pp. 439–475). New York: Springer.

Forlano, P. M., Sisneros, J. A., Rohmann, K. N., & Bass, A. H. (2015). Neuroendocrine control of seasonal plasticity in the auditory and vocal systems of fish. *Frontiers in Neuroendocrinology*, *37*, 129–145.

Fritzsch, B. (1999). Ontogenetic and evolutionary evidence for the motoneuron nature of vestibular and cochlear efferents. In C. Berlin (Ed.), *The efferent auditory system: Basic science and clinical applications* (pp. 31–60). San Diego, CA: Singular Publishing.

Funakoshi, K., Nakano, M., Atobe, Y., Kadota, T., Goris, R. C., & Kishida, R. (2002). Catecholaminergic innervation of the sympathetic preganglionic cell column of the filefish *Stephanolepis cirrhifer*. *The Journal of Comparative Neurology*, *442*, 204–216.

Furukawa, T. (1981). Effects of efferent stimulation on the saccule of goldfish. *The Journal of Physiology*, *315*, 203–215.

Furukawa, T., & Ishii, Y. (1967). Neurophysiological studies on hearing in goldfish. *Journal of Neurophysiology*, *30*, 1377–1403.

Garrett, A. R., Robertson, D., Sellick, P. M., & Mulders, W. H. A. M. (2011). The actions of dopamine receptors in the guinea pig cochlea. *Audiology & Neuro-otology*, *16*, 145–157.

Ghanem, T. A., Breneman, K. D., Rabbitt, R. D., & Brown, H. M. (2008). Ionic composition of endolymph and perilymph in the inner ear of the oyster toadfish, *Opsanus tau*. *The Biological Bulletin*, *214*, 83–90.

Gil-Loyzaga, P. E. (1995). Neurotransmitters of the olivocochlear lateral efferent system: With an emphasis on dopamine. *Acta Oto-laryngologica*, *115*, 222–226.

Goebrecht, G. K. E., Kowtoniuk, R. A., Kelly, B. G., & Kittelberger, J. M. (2014). Sexually-dimorphic expression of tyrosine hydroxylase immunoreactivity in the brain of a vocal fish (*Porichthys notatus*). *Journal of Chemical Neuroanatomy*, *56C*, 13–34.

Goodson, J. L., & Bass, A. H. (2002). Vocal–acoustic circuitry and descending vocal pathways in teleost fish: Convergence with terrestrial vertebrates reveals conserved traits. *The Journal of Comparative Neurology*, *448*, 298–322.

Guo, S., Brush, J., Teraoka, H., Goddard, A., Wilson, S. W., Mullins, M. C., & Rosenthal, A. (1999). Development of noradrenergic neurons in the zebrafish hindbrain requires BMP, FGF8, and the homeodomain protein Soulless/Phox2a. *Neuron*, *24*, 555–566.

Hama, K. (1969). A study on the fine structure of the saccular macula of the gold fish. *Zeitschrift Fu?r Zellforschung und Mikroskopische Anatomie (Vienna, Austria: 1948)*, *94*, 155–171.

Hama, K. (1978). A study of the fine structure of the pit organ of the common Japanese sea eel *Conger myriaster*. *Cell and Tissue Research*, *189*, 375–388.

Hama, K. (1980). Fine structure of the afferent synapse and gap junctions on the sensory hair cell in the saccular macula of goldfish: A freeze-fracture study. *Journal of Neurocytology*, *9*, 845–860.

Hama, K., & Saito, K. (1977). Gap junctions between the supporting cells in some acoustico-vestibular receptors. *Journal of Neurocytology*, *6*, 1–12.

Helfert, R. H., Juiz, J. M., Bledsoe, S. C., Bonneau, J. M., Wenthold, R. J., & Altschuler, R. A. (1992). Patterns of glutamate, glycine, and GABA immunolabeling in four synaptic terminal classes in the lateral superior olive of the guinea pig. *The Journal of Comparative Neurology*, *323*, 305–325.

Hnasko, T. S., Chuhma, N., Zhang, H., Goh, G. Y., Sulzer, D., Palmiter, R. D., … Edwards, R. H. (2010). Vesicular glutamate transport promotes dopamine storage and glutamate corelease in vivo. *Neuron*, *65*, 643–656.

Holzschuh, J., Ryu, S., Aberger, F., & Driever, W. (2001). Dopamine transporter expression distinguishes dopaminergic neurons from other catecholaminergic neurons in the developing zebrafish embryo. *Mechanisms of Development*, *101*, 237–243.

Hornby, P. J., & Piekut, D. T. (1990). Distribution of catecholamine-synthesizing enzymes in goldfish brains: Presumptive dopamine and norepinephrine neuronal organization. *Brain, Behavior and Evolution*, *35*, 49–64.

Jay, M., De Faveri, F., & McDearmid, J. R. (2015). Firing dynamics and modulatory actions of supraspinal dopaminergic neurons during zebrafish locomotor behavior. *Current Biology*, *25*, 435–444.

Jenkins, D. B. (1979). A transmission and scanning electron microscopic study of the saccule in five species of catfishes. *The American Journal of Anatomy*, *154*, 81–101.

Jordan, P. M., Fettis, M., & Holt, J. C. (2015). Efferent innervation of turtle semicircular cristae: Comparisons with bird and mouse. *The Journal of Comparative Neurology*, *523*, 1258–1280.

Kanoh, N. (1995). Dopamine inhibits the Na-K ATPase activity of the stria Vascularis in the cochlea: *In vivo* ultracytochemical study. *Acta Oto-laryngologica*, *115*, 27–30.

Kapsimali, M., Vidal, B., González, A., Dufour, S., & Vernier, P. (2000). Distribution of the mRNA encoding the four dopamine D1 receptor subtypes in the brain of the European eel (*Anguilla anguilla*): Comparative approach to the function of D1 receptors in vertebrates. *The Journal of Comparative Neurology*, *419*, 320–343.

Kaslin, J., & Panula, P. (2001). Comparative anatomy of the histaminergic and other aminergic systems in zebrafish (*Danio rerio*). *The Journal of Comparative Neurology*, *440*, 342–377.

Katz, E., Elgoyhen, A. B., & Fuchs, P. A. (2011). Cholinergic inhibition of hair cells. In D. K. Ryugo, R. R. Fay, & A. N. Popper (Eds.), *Auditory and vestibular efferents* (pp. 103–133). New York: Springer.

Khan, K. M., Drescher, M. J., Hatfield, J. S., & Drescher, D. G. (1993). Acetylcholinesterase activity is associated with efferent endings in the sensory epithelia of the utricle and semicircular canals of the rainbow trout inner ear. *The Anatomical Record*, *237*, 141–147.

Khan, K. M., Hatfield, J. S., Drescher, M. J., & Drescher, D. G. (1991). The histochemical localization of acetylcholinesterase in the rainbow trout saccular macula by electron microscopy. *Neuroscience Letters*, *131*, 109–112.

Köppl, C. (2011). Evolution of the octavolateral efferent system. In D. K. Ryugo, R. R. Fay, & A. N. Popper (Eds.), *Auditory and vestibular efferents* (pp. 217–259). New York: Springer.

Lanford, P. J., & Popper, A. N. (1996). Novel afferent terminal structure in the crista ampullaris of the goldfish, *Carassius auratus*. *The Journal of comparative Neurology*, *366*, 572–579.

Lendvai, B., Halmos, G. B., Polony, G., Kapocsi, J., Horváth, T., Aller, M., … Zelles, T. (2011). Chemical neuroprotection in the cochlea: The modulation of dopamine release from lateral olivocochlear efferents. *Neurochemistry International*, *59*, 150–158.

López, J. M., Perlado, J., Morona, R., Northcutt, R. G., & González, A. (2013). Neuroanatomical organization of the cholinergic system in the central nervous system of a basal actinopterygian fish, the Senegal Bichir *Polypterus senegalus*. *The Journal of Comparative Neurology*, *521*, 24–49.

Ma, P. M. (1994). Catecholaminergic systems in the zebrafish. I. Number, morphology, and histochemical characterisitics of neurons in the locus coeruleus. *The Journal of Comparative Neurology*, *344*, 242–255.

Ma, P. M. (1997). Catecholaminergic systems in the zebrafish. III. Organization and projection pattern of medullary dopaminergic and noradrenergic neurons. *The Journal of Comparative Neurology*, *381*, 411–427.

Maison, S. F, Liu, X. P., Eatock, R. A., Sibley, D. R., Grandy, D. K., & Liberman, M. C. (2012). Dopaminergic signaling in the cochlea: Receptor expression patterns and deletion phenotypes. *The Journal of neuroscience: The Official Journal of the Society for Neuroscience*, *32*, 344–355.

Marín, O., Smeets, W. J., & González, A. (1997). Distribution of choline acetyltransferase immunoreactivity in the brain of anuran (*Rana perezi*, *Xenopus laevis*) and urodele (*Pleurodeles waltl*) amphibians. *The Journal of Comparative Neurology*, *382*, 499–534.

McLean, D. L., & Fetcho, J. R. (2004). Ontogeny and innervation patterns of dopaminergic, norarenergic, and serotonergic neurons in larval zebrafish. *The Journal of comparative Neurology*, *480*, 38–56.

McMahon, D. G., Knapp, A. G., & Dowling, J. E. (1989). Horizontal cell gap junctions: Single-channel conductance and modulation by dopamine. *Proceedings of the National Academy of Sciences of the United States of America*, *86*, 7639–7643.

Medina, L., & Reiner, A. (1994). Distribution of choline acetyltransferase immunoreactivity in the pigeon brain. *The Journal of Comparative Neurology*, *342*, 497–537.

Moore, H., Fadel, J., Sarter, M., & Bruno, J. P. (1999). Role of accumbens and cortical dopamine receptors in the regulation of cortical acetylcholine release. *Neuroscience*, *88*, 811–822.

Mu, Y., Li, X. Q., Zhang, B., & Du, J. L. (2012). Visual input modulates audiomotor function via hypothalamic dopaminergic neurons through a cooperative mechanism. *Neuron*, *75*, 688-699.

Mueller, T., Vernier, P., & Wullimann, M. F. (2004). The adult central nervous cholinergic system of a neurogenetic model animal, the zebrafish *Danio rerio*. *Brain Research*, *1011*, 156–169.

Mulders, W. H. A. M., & Robertson, D. (2000). Morphological relationships of peptidergic and noradrenergic nerve terminals to olivocochlear neurones in the rat. *Hearing Research*, *144*, 53–64.

Mulders, W. H. A. M., & Robertson, D. (2005). Catecholaminergic innervation of guinea pig superior olivary complex. *Journal of Chemical Neuroanatomy*, *30*, 230–242.

Nakajima, Y., & Wang, D. W. (1974). Morphology of afferent and efferent synapses in hearing organ of goldfish. *The Journal of Comparative Neurology*, *156*, 403–416.

Nevue, A. A., Felix, II R. A., & Portfors, C. V. (2016). Dopaminergic projections of the subparafascicular thalamic nucleus to the auditory brainstem. *Hearing Research*, *341*, 202–209.

Pasqualini, C., Weltzien, F., Vidal, B., Baloche, S., Rouget, C., Gilles, N., … Dufour, S. (2009). Two distinct dopamine d2 receptor genes in the European eel: Molecular characterization, tissue-specific transcription, and regulation by sex steroids. *Endocrinology*, *150*, 1377–1392.

Pawlisch, B. A., Kelm-Nelson, C. A., Stevenson, S. A., & Riters, L. V. (2012). Behavioral indices of breeding readiness in female European starlings correlated with immunolabeling for catecholamine markers in brain areas involved in sexual motivation. *General and Comparative Endocrinology*, *179*, 359–368.

Pereda, A., Triller, A., Korn, H., & Faber, D. S. (1992). Dopamine enhances both electrotonic coupling and chemical excitatory postsynaptic potentials at mixed synapses. *Proceedings of the National Academy of Sciences of the United States of America*, *89*, 12088–12092.

Pérez, S. E., Yáñez, J., Marín, O., Anadón, R., González, A., & Rodríguez-Moldes, I. (2000). Distribution of choline acetyltransferase (ChAT) immunoreactivity in the brain of the adult trout and tract-tracing observations on the connections of the nuclei of the isthmus. *The Journal of Comparative Neurology*, *428*, 450–474.

Peters, A., & Palay, S. L. (1996). The morphology of synapses. *Journal of Neurocytology*, *25*, 687–700.

Peters, A., Palay, S. L., & Webster, H. F. (1991). *The fine structure of the nervous system: The neurons and supporting cells* (3rd ed.). Oxford: Oxford University Press.

Petersen, C. L., Timothy, M., Kim, D. S., Bhandiwad, A. A., Mohr, R. A., Sisneros, J. A., & Forlano, P. M. (2013). Exposure to advertisement calls of reproductive competitors activates vocal-acoustic and catecholaminergic neurons in the plainfin midshipman fish, *Porichthys notatus*. *PLoS One*, *8*, e70474.

Peute, J., Schild, R. G., Schild, V. A., Buijs, R. M., van Asselt, L. A. C., & van Oordt, P. G.W. J. (1987). Immunocytochemical evidence for peptidergic (GnRH) and dopaminergic innervation of the gonadotropic cells in the pituitary of the African catfish, *Clarias gariepinus*. *General and Comparative Endocrinology*, *67*, 303–310.

Pickel, V. M., Nirenberg, M. J., & Milner, T. A. (1996). Ultrastructural view of central catecholaminergic transmission: Immunocytochemical localization of synthesizing enzymes, transporters and receptors. *Journal of Neurocytology*, *25*, 843–856.

Pierre, J., Mahouche, M., Suderevskaya, E. I., Repérant, J., & Ward, R. (1997). Immunocytochemical localization of dopamine and its synthetic enzymes in the central nervous system of the lamprey *Lampetra fluviatilis*. *The Journal of Comparative Neurology*, *380*, 119–d135.

Pombal, M. A., Marín, O., & González, A. (2001). Distribution of choline acetyltransferase-immunoreactive structures in the lamprey brain. *The Journal of Comparative Neurology*, *431*, 105–126.

Popper, A. N., & Fay, R. R. (1999). The auditory periphery in fishes. In R. R. Fay & A. N. Popper (Eds.), *Comparative hearing: Fish and amphibians* (pp. 43–100). New York: Springer.

Popper, A. N., & Saidel, W. M. (1990). Variations in receptor cell innervation in the saccule of a teleost fish ear. *Hearing Research*, *46*, 211–227.

Roberts, B. L., & Meredith, G. E. (1992). The efferent innervation of the ear: Variations on an enigma. In D. B. Webster, A. N. Popper, & R. R. Fay (Eds.), *The evolutionary biology of hearing* (pp. 185–210). New York: Springer.

Robertson, D. (2009). Centrifugal control in mammalian hearing. *Clinical and Experimental Pharmacology & Physiology*, *36*, 603–611.

Rodríguez-Moldes, I., Molist, P., Adrio, F., Pombal, M. A., Yanez, S. E., Mandado, M., … Anadón, R. (2002). Organization of cholinergic systems in the brain of different fish groups: A comparative analysis. *Brain Research Bulletin*, *57*, 331–334.

Rohmann, K. N., & Bass, A. H. (2011). Seasonal plasticity of auditory hair cell frequency sensitivity correlates with plasma steroid levels in vocal fish. *The Journal of Experimental Biology*, *214*, 1931–1942.

Rohmann, K. N., Fergus, D. J., & Bass, A. H. (2013). Plasticity in ion channel expression underlies variation in hearing during reproductive cycles. *Current Biology: CB*, *23*, 678–683.

Roubert, C., Sagné, C., Kapsimali, M., Vernier, P., Bourrat, F., & Giros, B. (2001). A Na^+/Cl^- -dependent transporter for catecholamines, identified as a norepinephrine transporter, is expressed in the brain of the teleost fish medaka (*Oryzias latipes*). *Molecular Pharmacology*, *60*, 462–473.

Ruel, J., Nouvian, R., d'Aldin, C., Pujol, R., Eybalin, M., & Puel, J. L. (2001). Dopamine inhibition of auditory nerve activity in the adult mammalian cochlea. *The European Journal of Neuroscience*, *14*, 977–986.

Saidel, W. M., Popper, A. N., & Chang, J.S. (1990). Spatial and morphological differentiation of trigger zones in afferent fibers to the teleos utricle. *The Journal of Comparative Neurology*, *302*, 629–642.

Sans, A., & Highstein, S. M. (1984). New ultrastructural features in the vestibular labyrinth of the toadfish, *Opsanus tau*. *Brain Research*, *308*, 191–195.

Sas, E., Maler, L., & Tinner, B. (1990). Catecholaminergic systems in the brain of a gymnotiform teleost fish: An immunohistochemical study. *The Journal of Comparative Neurology*, *292*, 127–162.

Schweitzer, J., Lohr, H., Filippi, A., & Driever, W. (2012). Dopaminergic and noradrenergic circuit development in zebrafish. *Developmental Neurobiology*, *72*, 256–268.

Simmons, D. D. (2002). Development of the inner ear efferent system across vertebrate species. *Journal of Neurobiology*, *53*, 228–250.

Sisneros, J. A. (2007). Saccular potentials of the vocal plainfin midshipman fish, *Porichthys notatus*. *Journal of Comparative Physiology. A, Neuroethology, Sensory, Neural, and Behavioral Physiology*, *193*, 413–424.

Sisneros, J. A., & Bass, A. H. (2003). Seasonal plasticity of peripheral auditory frequency sensitivity. *The Journal of Neuroscience: The Official Journal of the Society for Neuroscience*, *23*, 1049–1058.

Sisneros, J. A., Forlano, P. M., Deitcher, D. L., & Bass, A. H. (2004). Steroid-dependent auditory plasticity leads to adaptive coupling of sender and receiver. *Science*, *305*, 405–407.

Smeets, W. J., & González, A. (2000). Catecholamine systems in the brain of vertebrates: New perspectives through a comparative approach. *Brain Research. Brain Research Reviews*, *33*, 308–379.

Smith, D. W., & Keil, A. (2015). The biological role of the medial olivocochlear efferents in hearing: Separating evolved function from exaptation. *Frontiers in Systems Neuroscience*, *9*, 12.

Sokolowski, B. H. A., & Popper, A. N. (1988). Transmission electron microscopic study of the saccule in the embryonic, larval, and adult toadfish *Opsanus tau*. *Journal of Morphology*, *198*, 49–69.

Sugihara, I. (2001). Efferent innervation in the goldfish saccule examined by acetylcholinesterase histochemistry. *Hearing Research*, *153*, 91–99.

Sun, W., & Salvi, R. (2001). Dopamine modulates sodium currents in cochlear spiral ganglion neurons. *NeuroReport*, *12*, 803–807.

Tay, T. L., Ronneberger, O., Ryu, S., Nitschke, R., & Driever, W. (2011). Comprehensive catecholaminergic projectome analysis reveals single-neuron integration of zebrafish ascending and descending dopaminergic systems. *Nature Communications*, *2*, 171.

Terreros, G., Jorratt, P., Aedo, C., Elgoyhen, A. B., & Delano, P. H. (2016). Selective attention to visual stimuli using auditory distractors is altered in alpha-9 nicotinic receptor subunit knock-out mice. *Journal of Neuroscience*, *36*, 7198–7209.

Thompson, A. M., & Thompson, G. C. (1995). Light microscopic evidence of serotoninergic projections to olivocochlear neurons in the bush baby (*Otolemur garnettii*). *Brain Research*, *695*, 263–266.

Tomchik, S. M., & Lu, Z. (2006a). Auditory physiology and anatomy of octavolateral efferent neurons in a teleost fish. *Journal of Comparative Physiology. A, Neuroethology, Sensory, Neural, and Behavioral Physiology*, *192*, 51–67.

Tomchik, S. M., & Lu, Z. (2006b). Modulation of auditory signal-to-noise ratios by efferent stimulation. *Journal of Neurophysiology*, *95*, 3562–3570.

Tsuneoka, Y., Maruyama, T., Yoshida, S., Nishimori, K., Kato, T., Numan, M., & Kuroda, K. O. (2013). Functional, anatomical, and neurochemical differentiation of medial preoptic area subregions in relation to maternal behavior in the mouse. *The Journal of Comparative Neurology*, *521*, 1633–1663.

Toro, C., Trapani, J. G., Pacentine, I., Maeda, R., Sheets, L., Mo, W., & Nicolson, T. (2015). Dopamine modulates the activity of sensory hair cells. *The Journal of Neuroscience: The Official Journal of the Society for Neuroscience*, *35*, 16494–16503.

Valdés-Baizabal, C., Soto, E., & Vega, R. (2015). Dopaminergic modulation of the voltage-gated sodium current in the cochlear afferent neurons of the rat. *PLoS One*, *10*, e0120808.

Weeg, M. S., Land, B. R., & Bass, A. H. (2005). Vocal pathways modulate efferent neurons to the inner ear and lateral line. *The Journal of Neuroscience: The Official Journal of the Society for Neuroscience*, *25*, 5967–5974.

Wegner, N. (1982). A qualitative and quantitative study of a sensory epithelium in the inner ear of a fish (*Colisa labiosa*; Anabantidae). *Acta Zoologica et Pathologica Antverpiensia*, *63*, 133–146.

Wibowo, E., Brockhausen, J., & Köppl, C. (2009). Efferent innervation of the auditory basilar papilla of scincid lizards. *The Journal of Comparative Neurology*, *516*, 74–85.

Woods, C. I., & Azeredo, W. J. (1999). Noradrenergic and serotonergic projections to the superior olive: Potential for modulation of olivocochlear neurons. *Brain Research*, *836*, 9–18.

Yamamoto, K., & Vernier, P. (2011). The evolution of dopamine systems in chordates. *Frontiers in Neuroanatomy*, *5*, 21.

Yazulla, S., & Studholme, K. M. (1995). Volume transmission of dopamine may modulate light-adaptive plasticity of horizontal cell dendrites in the recovery phase following dopamine depletion in goldfish retina. *Visual Neuroscience*, *12*, 827–836.

Zaccone, G., Abelli, L., Salpietro, L., Zaccone, D., Manganaro, M., & Marino, F. (2011). Immunolocalization of neuotransmitter-synthesizing enzyymes and neuropeptides with associated receptors in the photophores of the hachetfish, *Argyropelecus hemigymnus* Cocco, 1829. *Acta Histochemica*, *113*, 457–464.

Zhang, S., Qi, J., Li, X., Wang, H. L., Britt, J. P., Hoffman, A. F., … Morales, M. (2015). Dopaminergic and glutamatergic microdomains in a subset of rodent mesoaccumbens axons. *Nature Neuroscience*, *18*, 386–392.

Zhu, Y., Liang, C., Chen, J., Zong, L., Chen, G.D., & Zhao, H. B. (2013). Active cochlear amplification is dependent on supporting cell gap junctions. *Nature Communications*, *4*, 1786.

How to cite this article: Perelmuter JT, Forlano PM. Connectivity and ultrastructure of dopaminergic innervation of the inner ear and auditory efferent system of a vocal fish. *J Comp Neurol*. 2017;00:000–000. https://doi.org/10.1002/cne.24177